

Electronics for cryogenic detectors for particle physics

Gianlugi Pessina
INFN Milano Bicocca
Università di Milano Bicocca



pessina@mib.infn.it, <http://pessina.mib.infn.it>

- Preamble;
- The base for the choice of the front-end configuration;
- Frontend for Low impedance Cryogenic Detectors;
- Frontend for Medium and High impedance Cryogenic Detectors;.

Preamble: Electronics for cryogenic particle detectors

Take care:

This text colour is for general discussion...

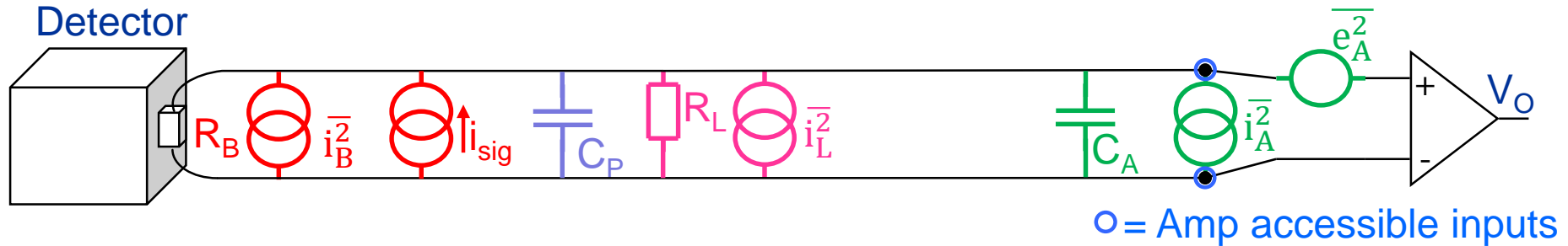
This text colour is related to circuit design, mainly...

Index: The base for the choice of the front-end configuration;

- Preamble;
- The base for the choice of the front-end configuration;
- Frontend for Low impedance Cryogenic Detectors;
- Frontend for Medium and High impedance Cryogenic Detectors;.

Noise sources vs configuration

Regardless the feedback configuration, the intrinsic noise sources of the amplifier have always the same effects and the system can be modelled as:



R_B (or Z_B): detector impedance;

i_B^2 : detector noise;

i_{sig} : detector signal;

C_P : parasitic capacitance;

R_L : biasing resistor;

i_L^2 : R_L 's parallel noise;

C_A : amplifier input capacitance;

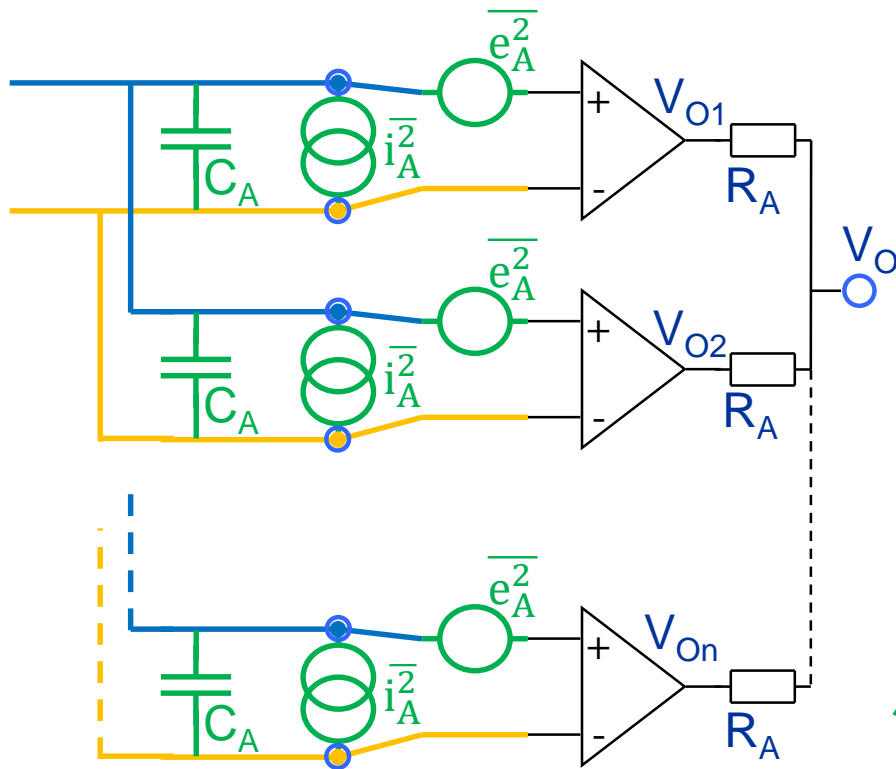
i_A^2 : amplifier parallel input noise;

e_A^2 : amplifier series input noise.

We must not forget the actors: input impedances of the preamplifier, detector, parasitic and load as well as noise sources.

...noise sources vs configuration 2

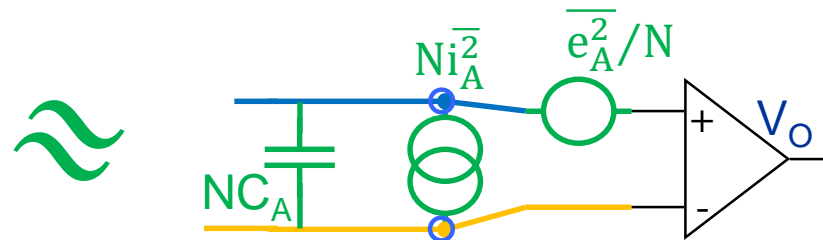
Once the devices technology has been chosen, there is a bit of flexibility that can be exploited by connecting in parallel several preamplifiers or, better, adjust the area of the transistor at the input of the preamplifier.



The output is the average of each preamplifier.

Since each series noise source generates an independent effect, they are averaged. This is not the case for parallel noise since each source develops its own effect across all inputs.

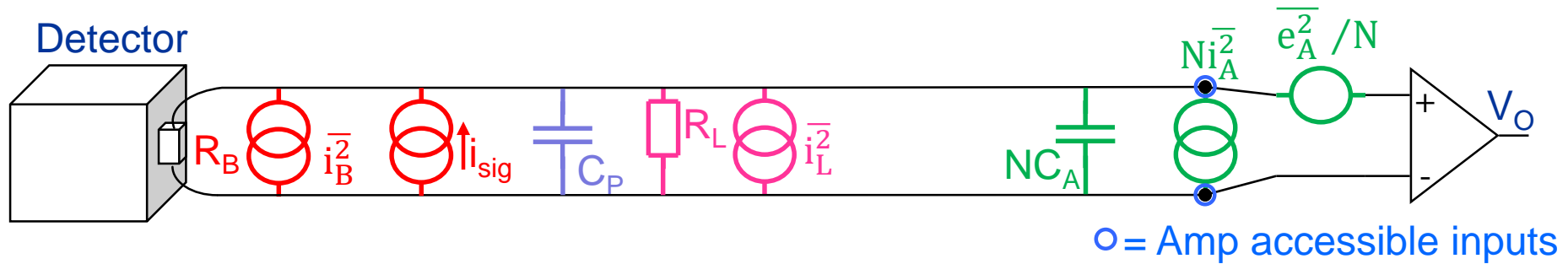
The equivalent model of the parallel combination is the preamplifier below:



The product $C_A \overline{e_A^2}$ has the dimension of an energy and is independent from the area selected for the transistor: it is a technological factor of merit.

Front-end optimization

Coming back to our scheme:



$$\overline{V_O^2(\omega)} = \frac{\overline{e_A^2}}{N} + \frac{(R_B \parallel R_L)^2}{1 + \omega^2(C_P + NC_A)^2(R_B \parallel R_L)^2} [\overline{i_B^2} + \overline{i_L^2} + N\overline{i_A^2}]$$

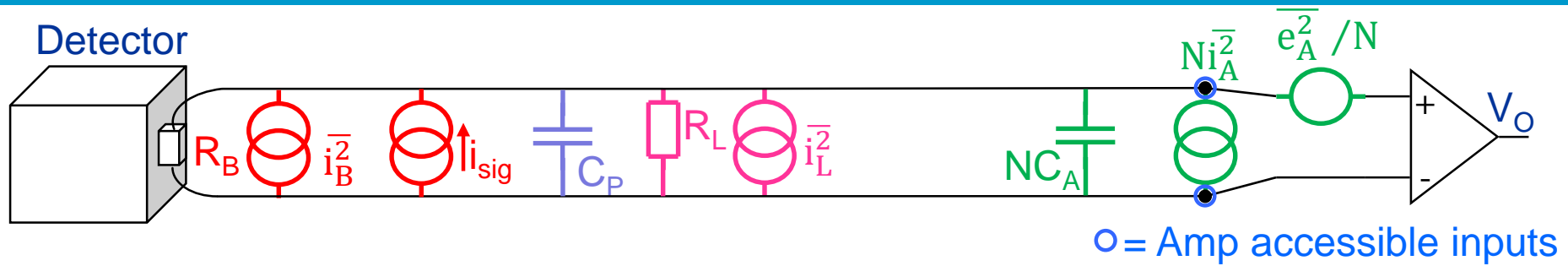
$$V_O(\omega) = \frac{R_B \parallel R_L}{1 + j\omega(C_P + NC_A)(R_B \parallel R_L)} i_{\text{sig}}(\omega)$$

The matched filter is the weigh of the S/N at each frequency: $F_M(\omega) = \frac{V_O^*(\omega)}{\overline{V_O^2(\omega)}}$

Under this condition the S/N is given by:

$$\frac{S^2}{N^2} = \int \frac{|V_O(\omega)|^2}{\overline{V_O^2(\omega)}} df = \int \frac{i_{\text{sig}}^2(\omega)}{\frac{1 + \omega^2(C_P + NC_A)^2(R_B \parallel R_L)^2}{(R_B \parallel R_L)^2} \frac{\overline{e_A^2}}{N} + \overline{i_B^2} + \overline{i_L^2} + N\overline{i_A^2}} df$$

... front-end optimization 2



N represents the area of the input transistor

$$\frac{S^2}{N^2} = \int \frac{i_{sig}^2(\omega)}{\underbrace{\frac{1 + \omega^2 (C_P + N C_A)^2 (R_B \parallel R_L)^2}{(R_B \parallel R_L)^2}}_{\text{Input impedance}} \left(\frac{\bar{e}_A^2}{N} + \bar{i}_B^2 + \bar{i}_L^2 + N \bar{i}_A^2 \right)} df$$

For large or small values of **N** the denominator of the S/N gets large values and the S/N itself reduces.

It exists an optimum for **N** that depends upon 2 main parameters:

- ✓ The impedance given by the parallel of $R_B \parallel R_L \parallel C_P \parallel C_A$;
- ✓ The signal bandwidth.

Feedback Topology and Front-end location

The topology of the very front-end can be based on:

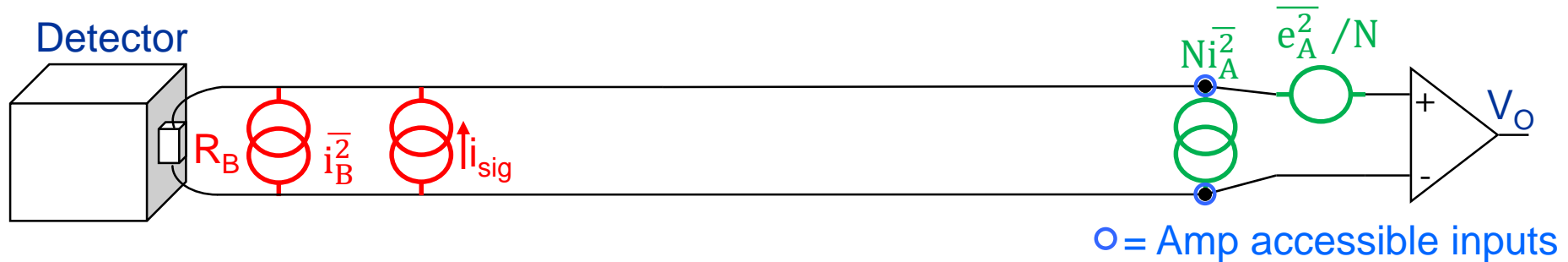
- ✓ Sensor impedance;
- ✓ Signal bandwidth;
- ✓ Number of channels;
- ✓ Rate of events;
- ✓ Front-end Location: at room or at cold;
- ✓ Budget background contribution from the material close to detector;
- ✓ ...

Index: Frontend for Low Impedance Cryogenic Detectors. LID

- Preamble;
- The base for the choice of the front-end configuration;
- Frontend for Low impedance Cryogenic Detectors;
- Frontend for Medium and High impedance Cryogenic Detectors.

Frontend for Low impedance Cryogenic Detectors

When the sensor is TES, MMC, MKID, the resistance is extremely small and we reduces to (R_L could come into play in some cases with squid) :



$$(i_{sig}(\omega) = \alpha F(\omega) U_{energy}) \quad \frac{S^2}{N^2} \approx \int_{\text{Signal Bw}} \frac{N \alpha^2 U_{energy}^2}{\frac{\overline{e_A^2}}{R_B^2} + N(\overline{i_B^2} + \overline{i_L^2} + N\overline{i_A^2})} df$$

In this case, the limit in the use of a cold stage is the power necessary to operate an amplifier with a large input transistor.

Power handling is less critical with a room temperature operated amplifier, but the signal at the amplifier input could be small and a boost is often needed...

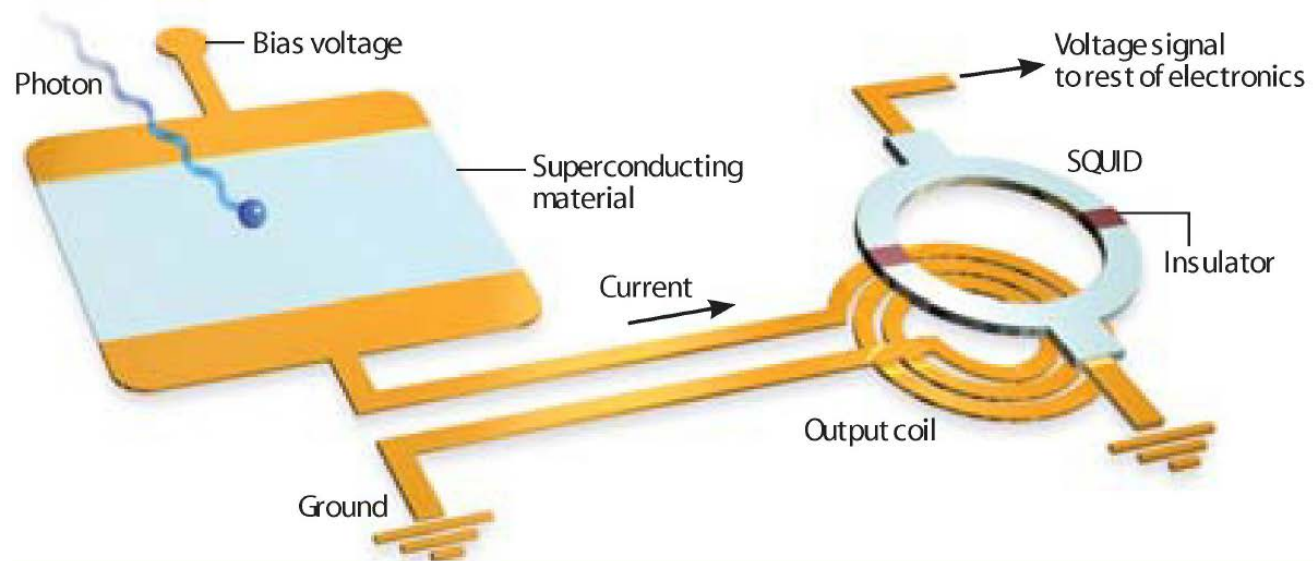
...anyway... there is a quite practical lower limit in the obtainable noise that is around 0.1 - 0.5 nV/ $\sqrt{\text{Hz}}$ at low frequency at room temperature, lower at high frequency at cold: the setups work practically always unmatched.

... frontend for low impedance cryogenic detectors 2

As we know, what that does signals manageable is the use of the SQUID, “the superconductor transformer”:



Josephson Effect to the rescue: amplification by SQUIDs



from Kent Irwin (NIST)

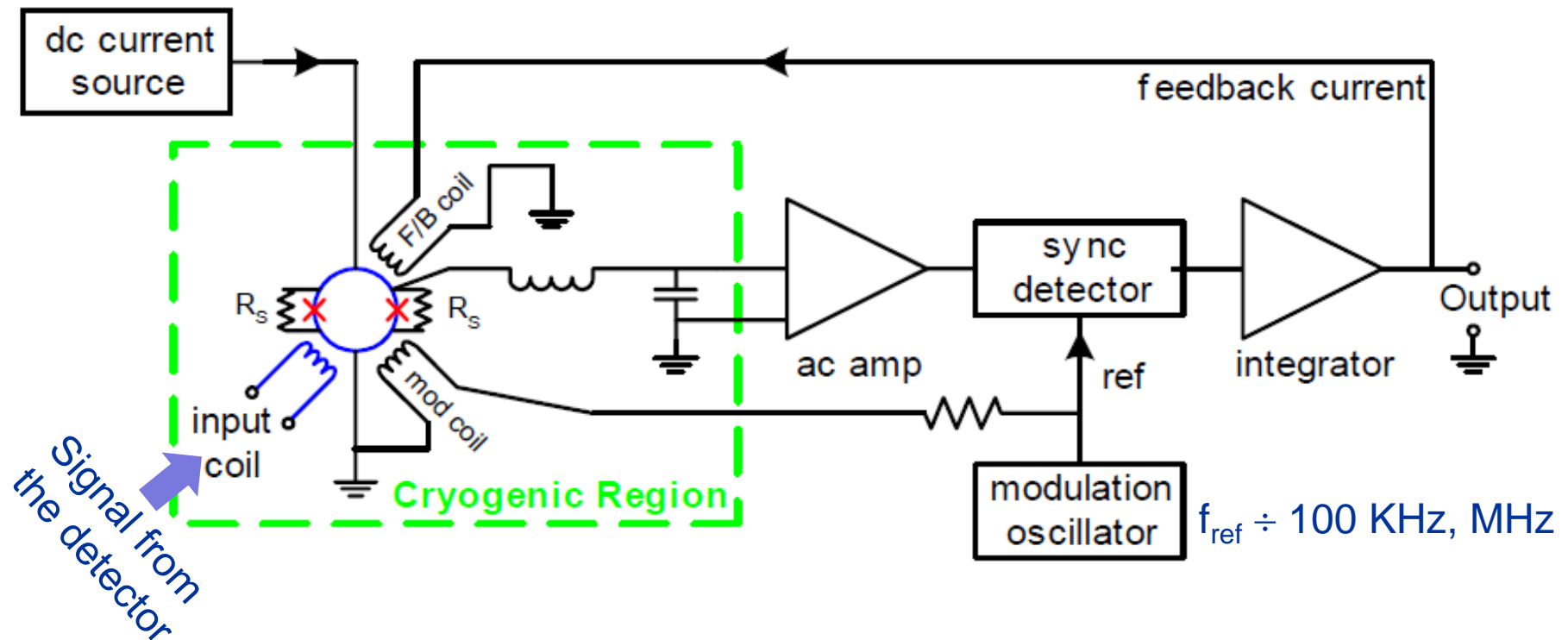
Story: Bell Labs
and NIST in the '60

There are 2 classes of squids:

- ✓ The dc squids are readout by room temperature preamplifier (and helped by transformers in some cases);
- ✓ The rf squids are readout by a cryogenic amplifier;

... frontend for LID: dc squid 4

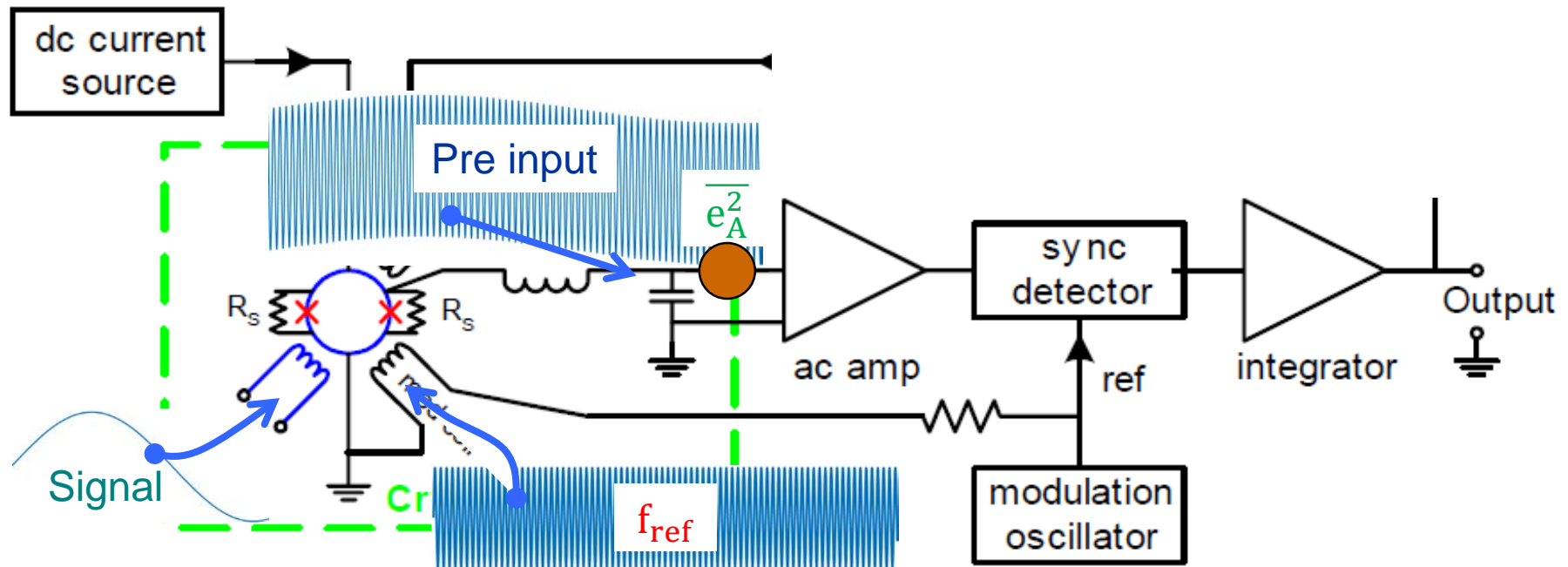
Entering a bit of details, dc squid (characterized by 2 Josephson junctions) are DC biased but are most of the time operated in closed loop with the so called FLL, **F**lux **L**ocked **L**oop.



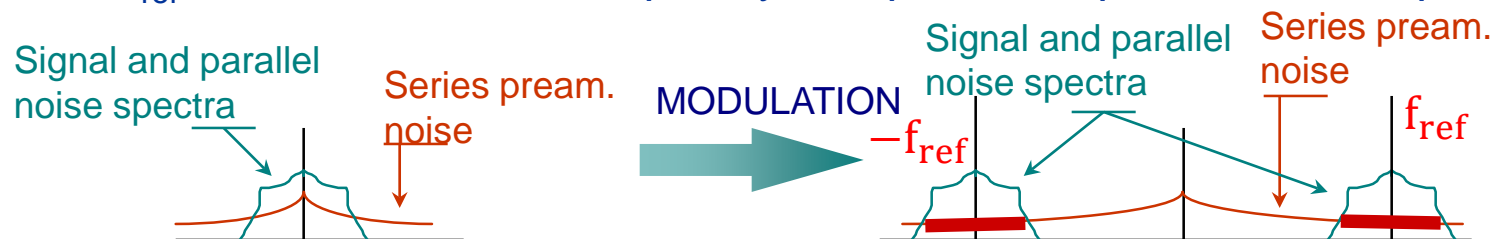
The FLL is a feedback that forces the flux within the squid almost constant by compensating the input flux from the sensor that modulates it: this way the squid is operated in a narrow region of its characteristics and the linearity is greatly improved.

... frontend for LID: dc squid 5

Very is another advantage in the modulation in general: if the reference modulation has a frequency \gg that of the input signal, the resulting preamplifier input is a modulation of the reference:



Preamplifier noise does not enter in the modulation business and its contribution is that around f_{ref} : therefore, its low-frequency component, if present, is swept away:



... frontend for LID: dc squid 6

The frequency at which the FLL operates is relatively small, from hundreds of KHz to few MHz and the front-end noise must be white: a standard is a room temperature operated front-end.

Front-end series noise is sub-nV/ $\sqrt{\text{Hz}}$, from 0.1 nV/ $\sqrt{\text{Hz}}$ to 1 nV/ $\sqrt{\text{Hz}}$. Parallel noise ranges from negligible values, for JFET input stage, to a few pA/ $\sqrt{\text{Hz}}$, bipolar input stage.

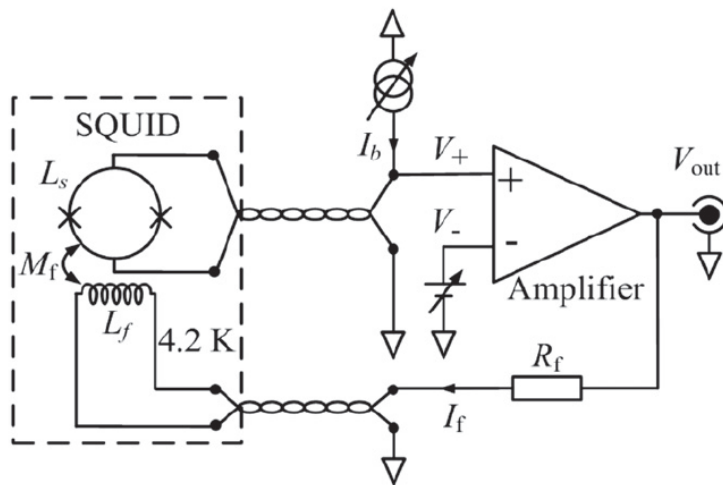


Figure 1. Equivalent circuit of SCRE with a current biased SQUID.
The AD797 operational amplifier is employed in our case.

Supercond. Sci. Technol. 2014, **27** 115004

This is a straightforward solution based on the use of only a well-known operational amplifier: the AD797 that features a nominal 0.9 nV/ $\sqrt{\text{Hz}}$ and 2 pA/ $\sqrt{\text{Hz}}$ (above 1 KHz).

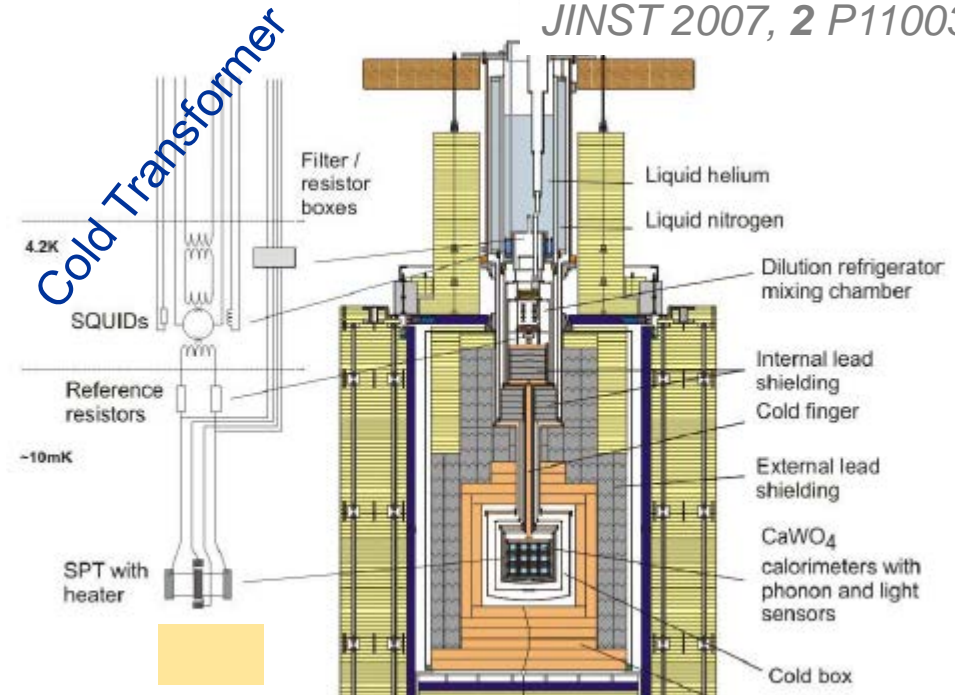
Authors claim a transfer coefficient $\partial V / \partial \Phi_0$ of about 380 $\mu\text{V} / \Phi_0$, that translates into a preamplifier noise contribution of less than 3 $\mu\Phi_0 / \sqrt{\text{Hz}}$ (squid intrinsic noise should be a fraction of $\mu\Phi_0 / \sqrt{\text{Hz}}$, $\Phi_0 = h / (2e) \approx 2.07 \times 10^{-15} \text{ Vs}$, the magnetic flux quantum).

... frontend for LID: dc squid 7

JINST 2007, 2 P11003

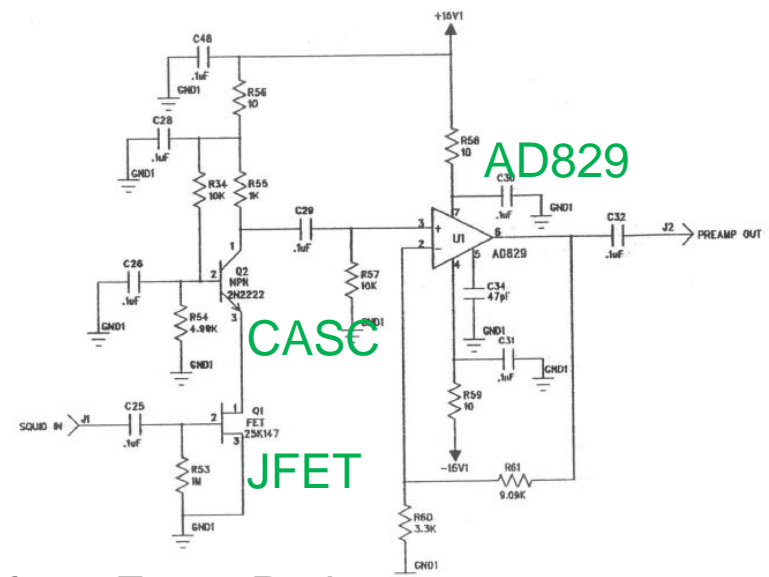
CRESST studies the Dark matter with an array of large mass CaWO_4 scintillating crystals sensed by TES.

CRESST runs are very long with a strict request on stability.
To maintain steady the energy conversion gain, each detector of the array is equipped with a heater to which a constant power and periodic pulses are sent.



The readout is with dc squid + transformer at cold (8:1) + transformer at room T (3:1) + room T amplifier (JFET input, 2SK147, with a noise floor of $0.7 \text{ nV}/\sqrt{\text{Hz}}$).

They claim a current noise close to that of the junction, $1.2 \text{ pA}/\sqrt{\text{Hz}}$, thanks to the great mitigation of the amplifier noise which comes from the 2 transformers.

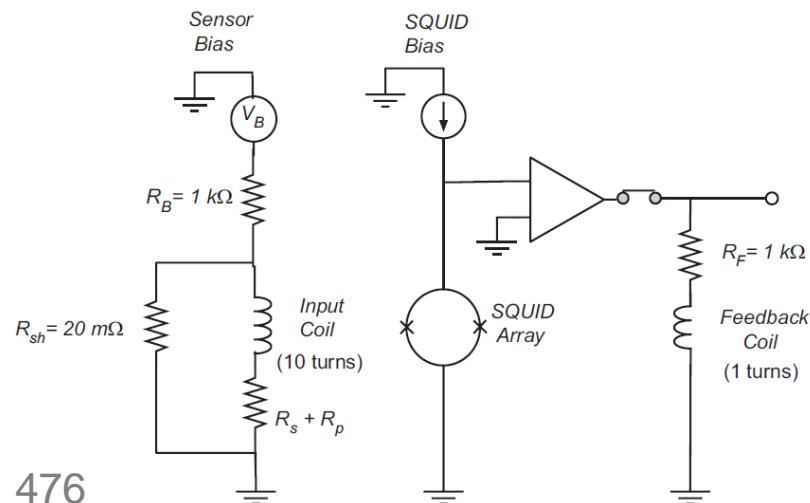
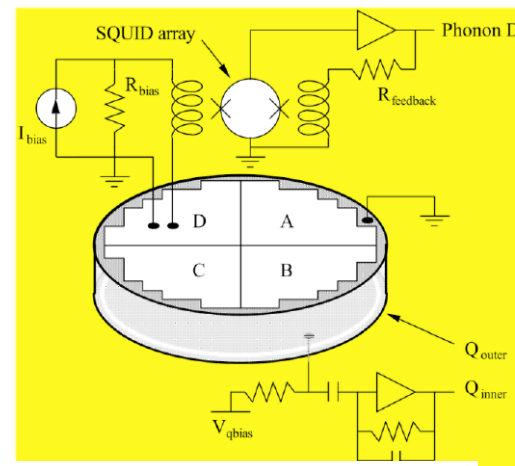


... frontend for LID: dc squid 8

SuperCDMS studies the Dark matter, too, with TES for the phonon channel.

The readout is with dc squid (a series of 100 squids to mitigate preamplifier noise contribution) + room temperature amplifier.

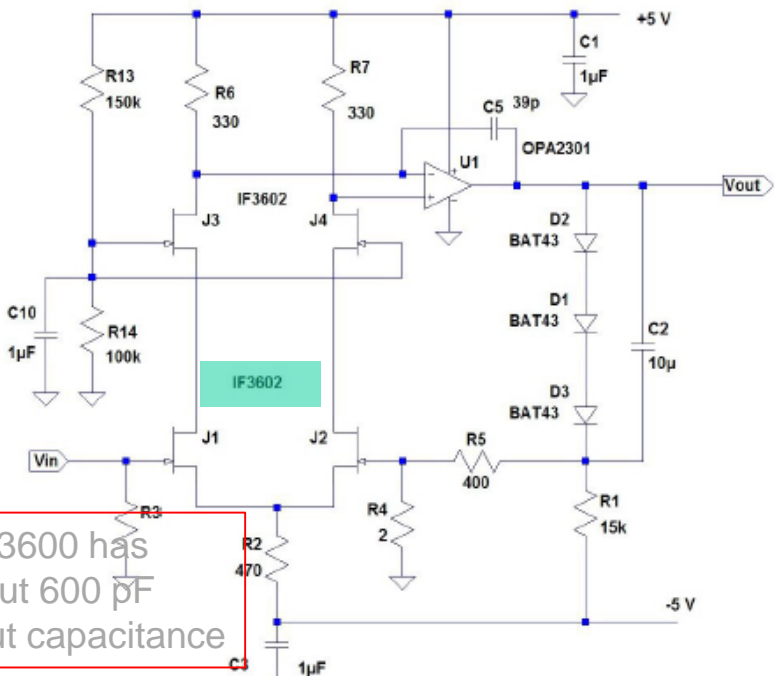
They claim a current noise close to about $10 \text{ pA}/\sqrt{\text{Hz}}$, with $1.2 \text{ nV}/\sqrt{\text{Hz}}$ being the series noise of the preamplifier.



NIMA 2008, 591, 476
AIP Con. Proc. **1185**, 282 (2009)

... frontend for LID: dc squid 9

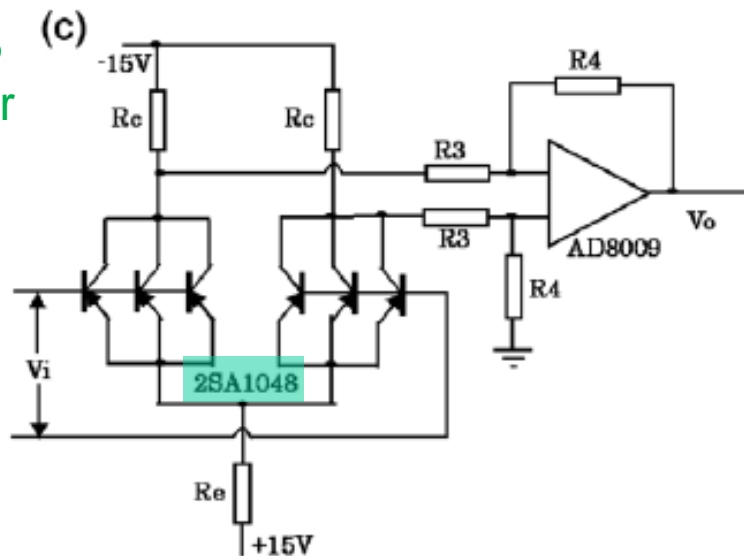
Here other examples of room temperature operated amplifiers: one with bipolar input ($0.35 \text{ nV}/\sqrt{\text{Hz}}$) and the other with JFET input transistor ($1 \text{ nV}/\sqrt{\text{Hz}}$ @ 300 K , $0.6 \text{ nV}/\sqrt{\text{Hz}}$ @ $-100 \text{ }^\circ\text{C}$).



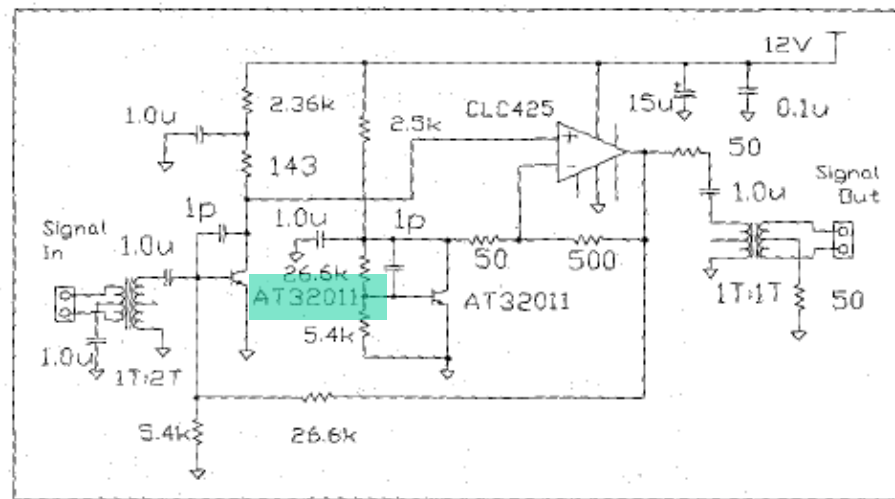
Proc. SPIE 9904, doi: 10.1117/12.2232859

Here a preamplifier operated at both room temperature and 125 K with a performance of about $5 \mu\Phi_0/\sqrt{\text{Hz}}$

LTD-18, gpressina



Physica C 445–448 (2006) 982–985



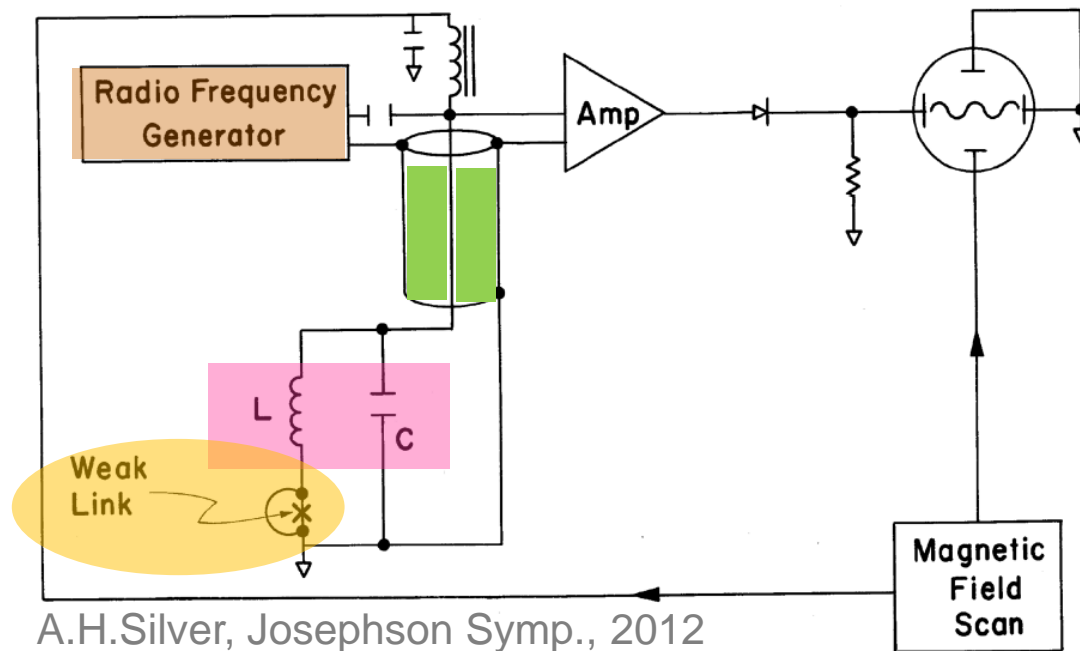
IEEE Tr. APP. SUPERCOND. 1997, 7, 2323

... frontend for LID: rf squid 10

The ingredients to operate an rf squid (characterized by 1 Josephson junction) are: the so called tank or tuned circuit, L and C, the transmission line to the front-end and the radio frequency generator.

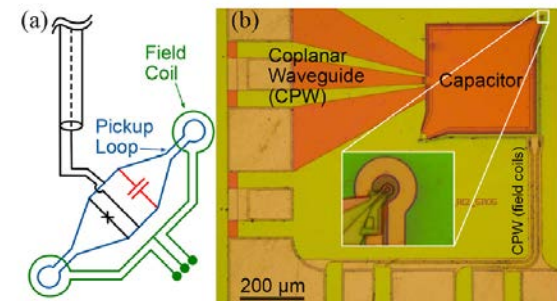
Large signals are obtained at large frequencies, large inductance and small capacitance, which conflict with the transmission line impedance matching requirement whenever the line is longer than $\lambda/2$.

Single Junction RF SQUID



At 30 MHz the wave length is a few meters, no problems with room temperature operated front-end, at 1 GHz the wave length is some centimetres: **need for a cryogenic stage.**

For resonating frequencies > 1 GHz squid and tank circuit are in a single chip:

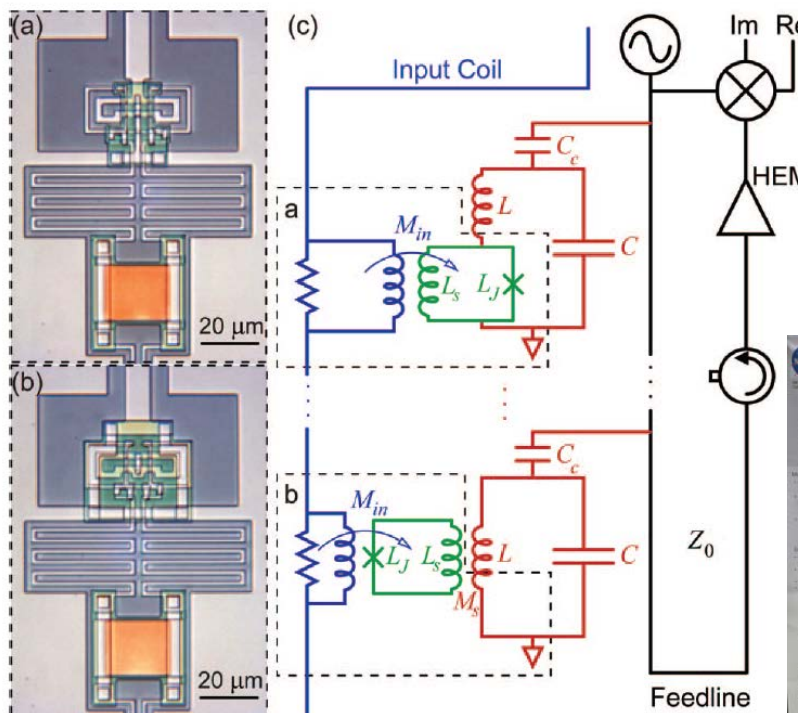


Appl. Phys. Lett. 112, 252601 (2018)

... frontend for LID: ac squid 13

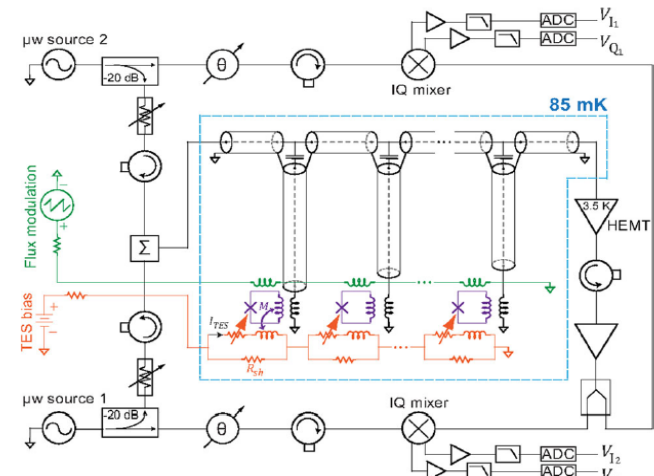
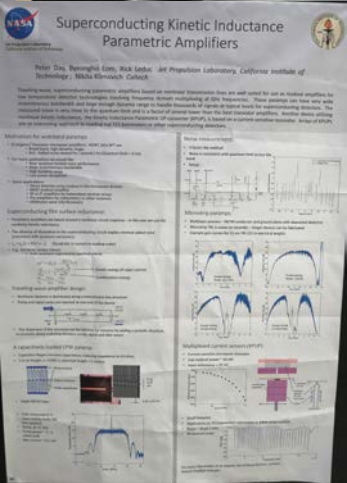
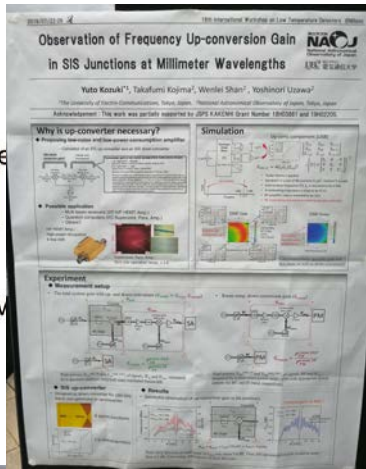
The tank circuit and the squid are side by side on the same chip. Changing the tuned frequency from squid to squid a single line can be exploited to send a superimposition of tones to an array. The same single line can be used for readout, too, and de-multiplexing is made by sw. The signal modulates the own tone.

Here arrays of TES sensors are coupled to arrays of rf squids ...

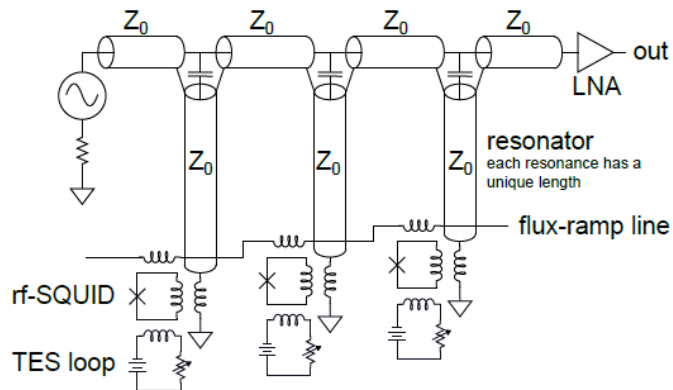


Appl. Phys. Lett. 92, 023514 2008

LTD-18, gpressina



Eur. Phys. J. C (2015) 75:112



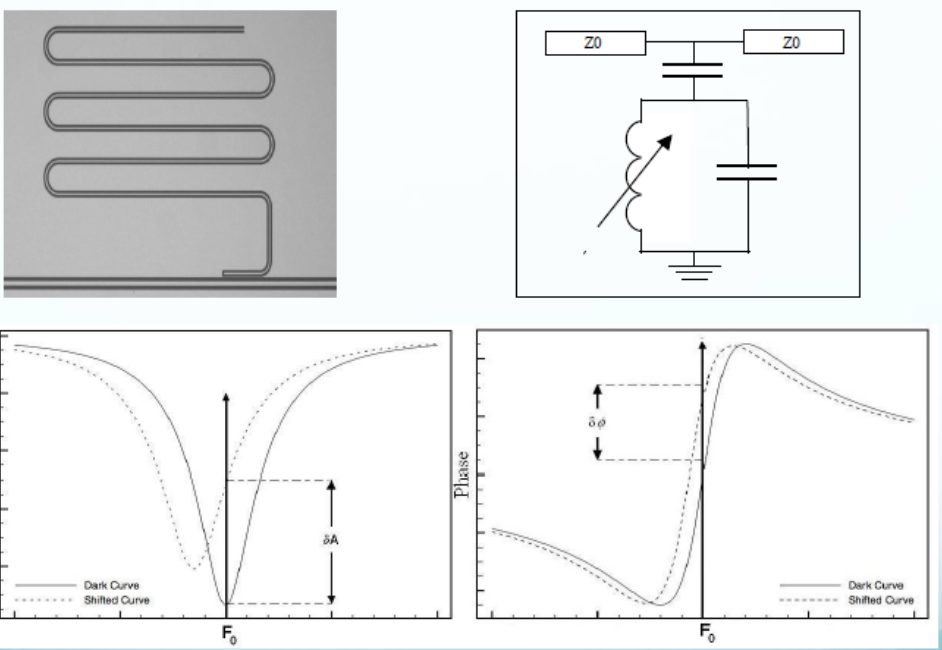
CMB-S4 Collaboration

... frontend for LID: MKID 14

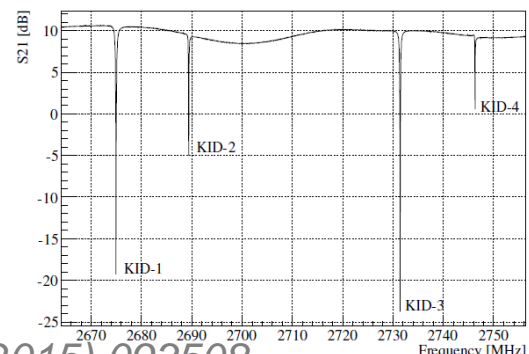
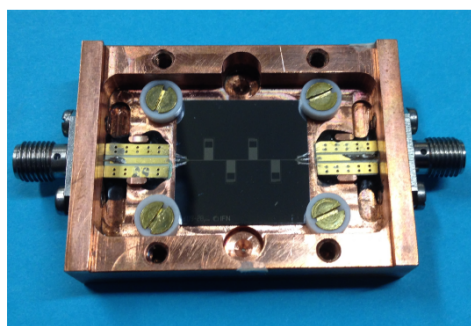
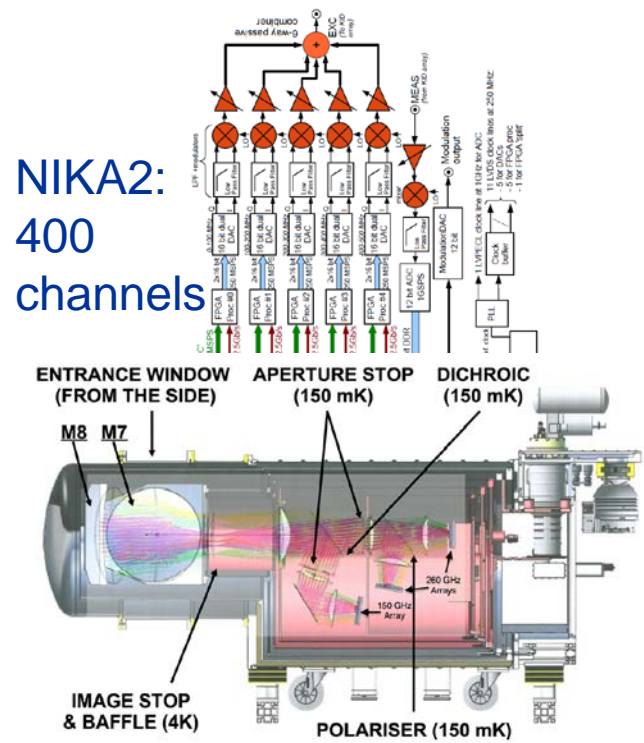
A sensor that can be multiplexed without the need of squids is the Microwave Kinetic Inductance Detector, MKID, a superconducting stub:

As soon as the MKID is subjected to a T change, its impedance changes, inducing a change in both the amplitude and phase of the applied tone.

The quarter wave resonator



NIKA2:
400
channels

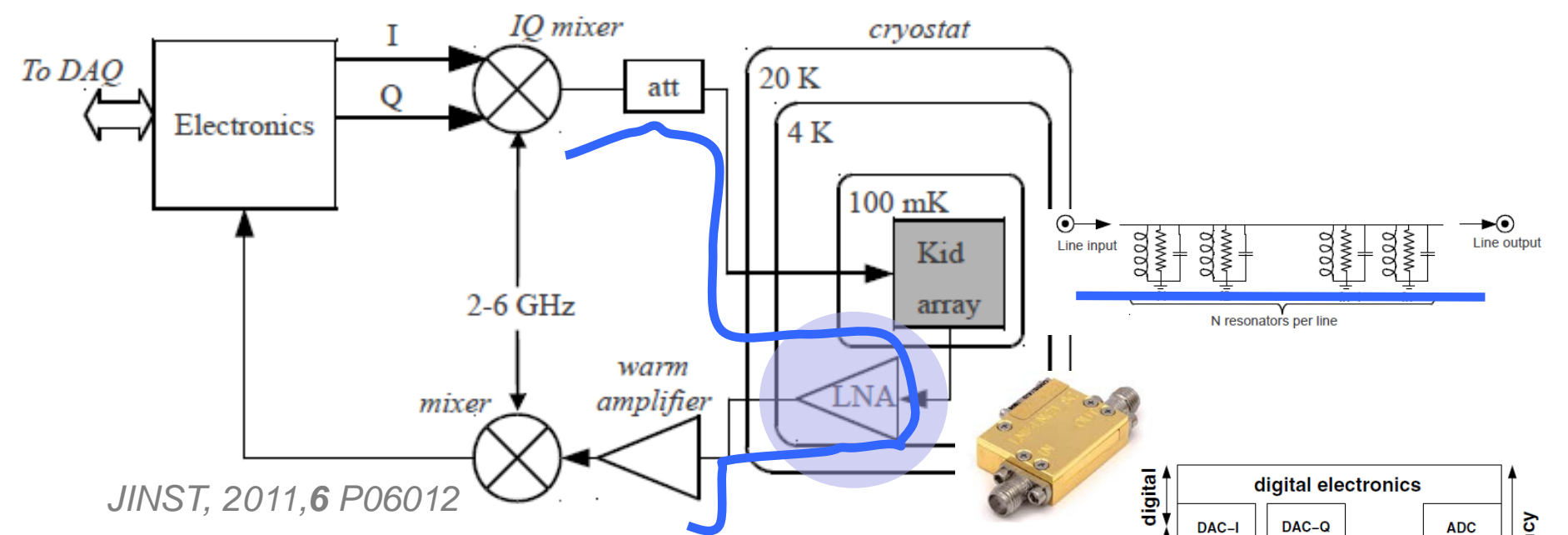


A&A 609, A115 (2018)
LTD-18, gpressina

APL 107 (2015) 093508

... frontend for LID: MKID 15

Both rf squid and MKID arrays can be multiplexed thanks to the use of a microwave cryogenic Low Noise Amplifier, LNA.



JINST, 2011, 6 P06012

Most of the times the LNA limits the achievable resolution. Nevertheless it does a great job working at and below 4.2 K.

Take care of the operating freq as the noise increases.

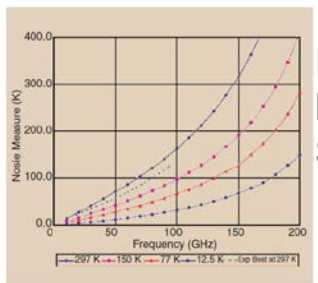
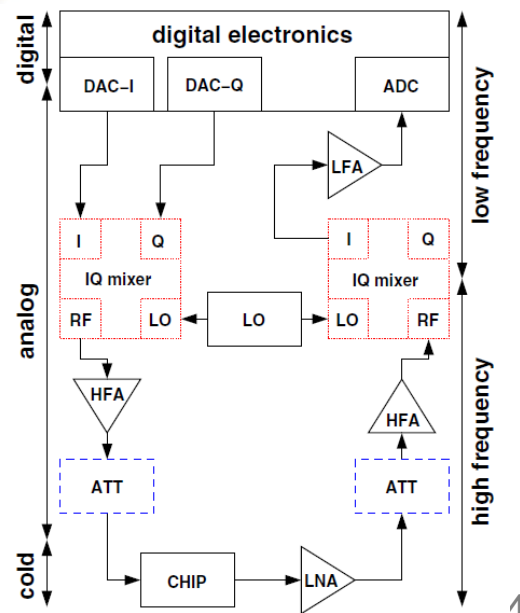


Figure 14. A minimum noise measure of 0.1-μm gate length AlInAs/GaInAs/InP HFET [38]. The best experimental results from different laboratories are also shown [72]–[74].

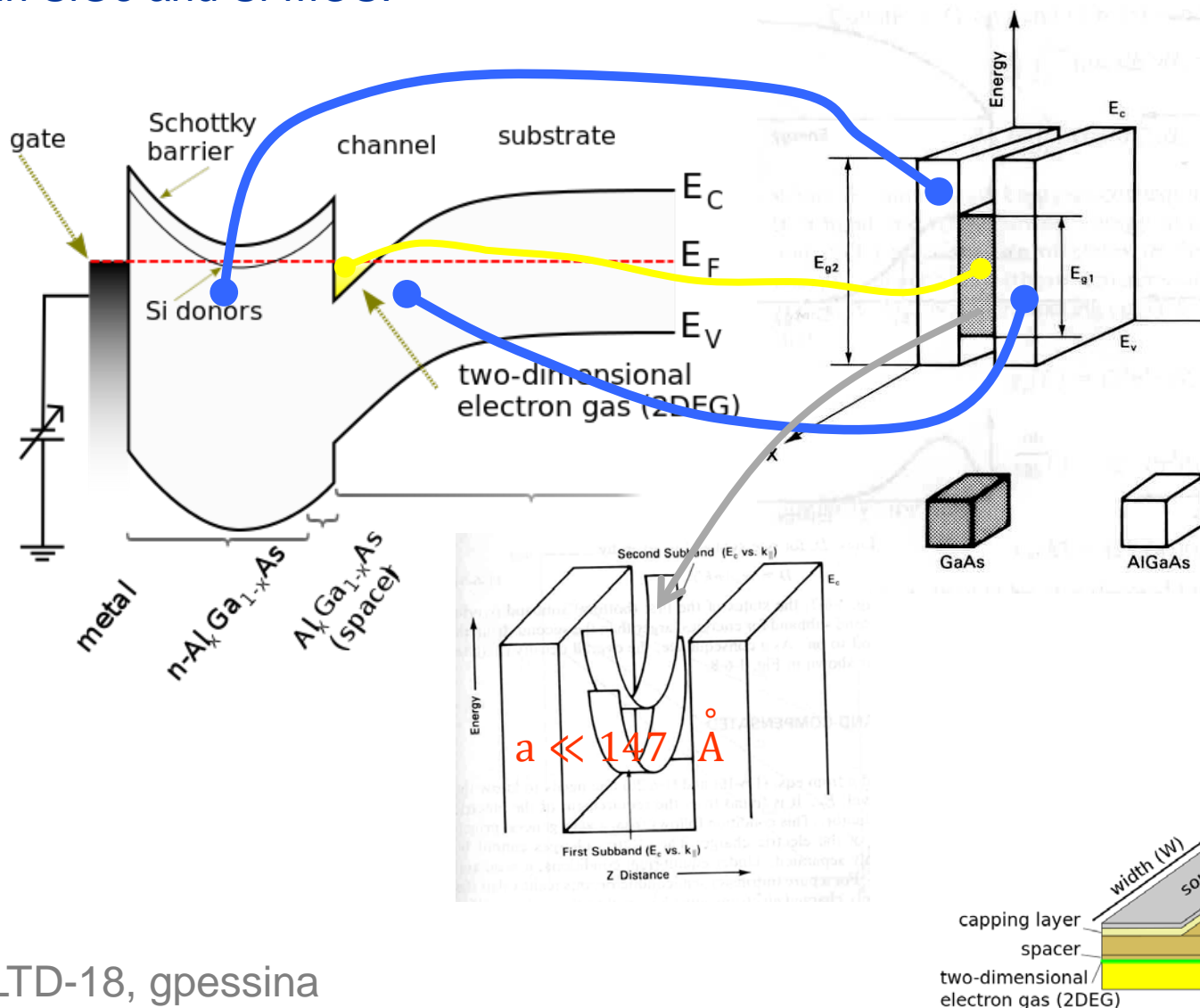
IEEE Microw. Mag., Sep, 2005



Eur. Phys. J. C (2015) 75:353

... frontend for LID: LNA technology 16

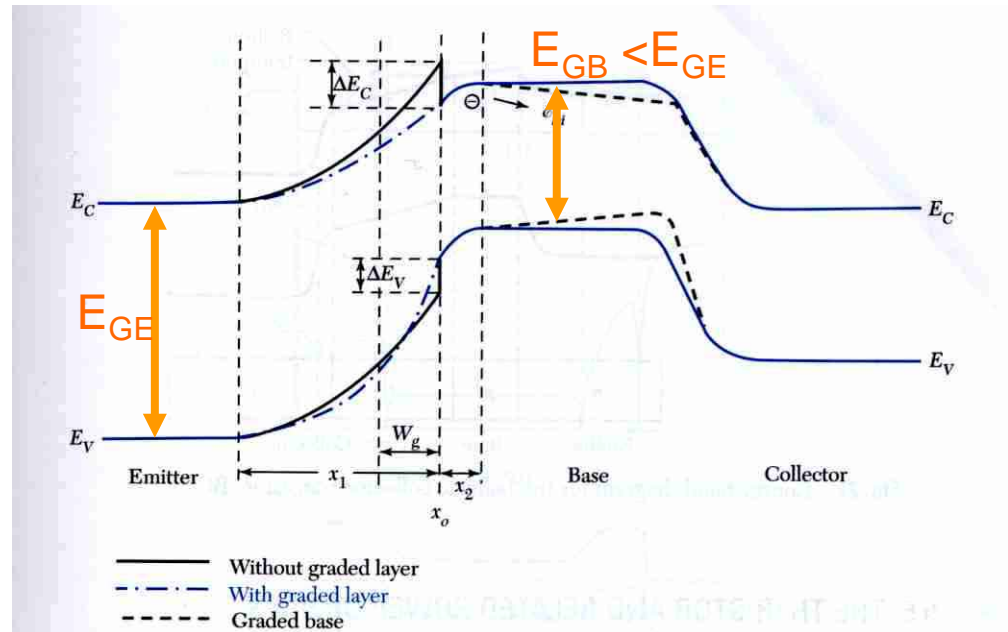
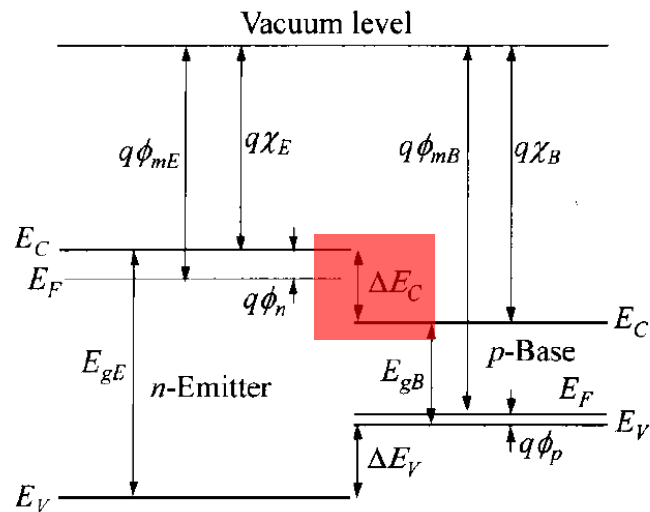
Devices able to work at so small temperature are those manufactured in III – V compound such as HEMT (InP, InGaAs, ...), MESFET in GaAs and AlGaAs and HBT in SiGe and Si-MOS.



The HEMT is a «sandwich» between 2 semiconductors with large bandgap and a 2D un-doped sheet with smaller bandgap. Electrons driven in the sheet from the applied gate voltage are quantized and move within it at very high speed at any temperature as there is no scattering.

... frontend for LID: LNA technology 17

The SiGe HBT has the p-base of smaller bandgap with respect to the emitter as a small percentage of Ge atoms are introduced to modify its nature.



This metallurgical modification of the base allows the diffusion of a high level of dopant concentration, which improves the speed, the gain and also the gain at low temperature (not verified for all...):

$$h_{FE} \doteq \frac{I_C}{I_B} \approx \frac{N_e}{P_b} \frac{n_{ib}^2}{n_{ie}^2} = \frac{N_e}{P_b} \exp\left(\frac{\Delta E_C}{K_B T}\right)$$

In conventional Si-bipolar the gain lowers with T as it is the emitter that has the bandgap smaller than that of the base: $h_{FE} \doteq \frac{I_C}{I_B} \approx \frac{N_e}{P_b} \exp\left(-\frac{\Delta E_{EB}}{K_B T}\right)$

... frontend for LID: LNA 18

Design and implementation of microwave amplifiers must follow well-defined rules which regard both the geometry of all the connections for obtaining proper terminations and the stability of the transistors that are otherwise prone to oscillate at high frequency.

Cryogenics 60 (2014) 76–79

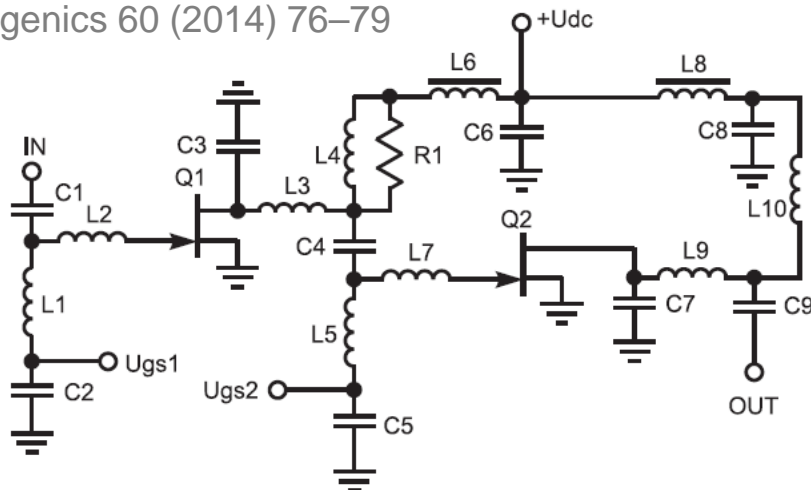
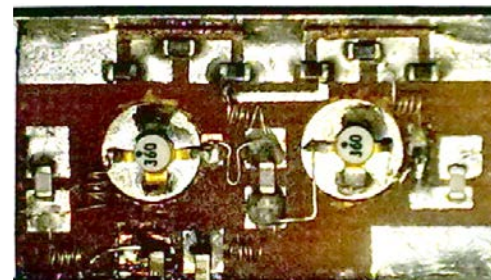
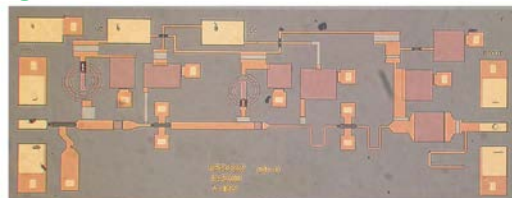
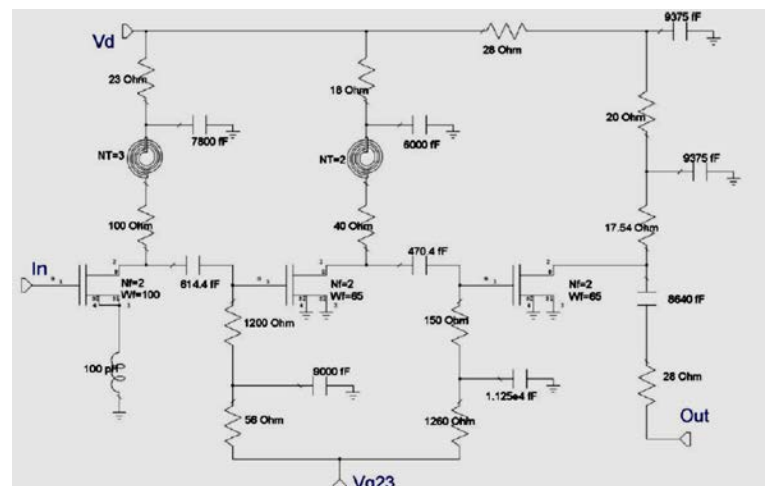


Fig. 2. The amplifier schematic. Q1, Q2 – ATF-36077.

This is a 3 stages common-source with inductance at the source of the input HEMT for matching.



The amplifier is a multistage common-source or common-emitter operated open loop.



... frontend for LID: LNA 19

A monolithic SiGe amplifier composed with the cascade of 2 common-emitter stages. The DC bias is made with 2 current mirrors which are decoupled by inductances.

Cryogenic microwave amplifiers are able to show less than $100 \text{ pV}/\sqrt{\text{Hz}}$ at the centre bandwidth, around a few GHz.

This correspond to about 2 K noise temperature (*), which for an rf squid transfer coefficient of $100 \mu\text{V}/\Phi_0$ gives about $1 \mu\Phi_0/\sqrt{\text{Hz}}$, with the noise floor of the rf squid that could be 5 – 10 times better.

Cascode SiGe.

(*) the noise of 50 Ω resistor held at the noise temperature, as a target.

DOI: 10.1109/BCTM.2011.6082758

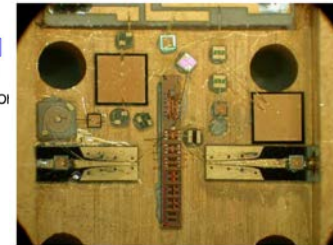
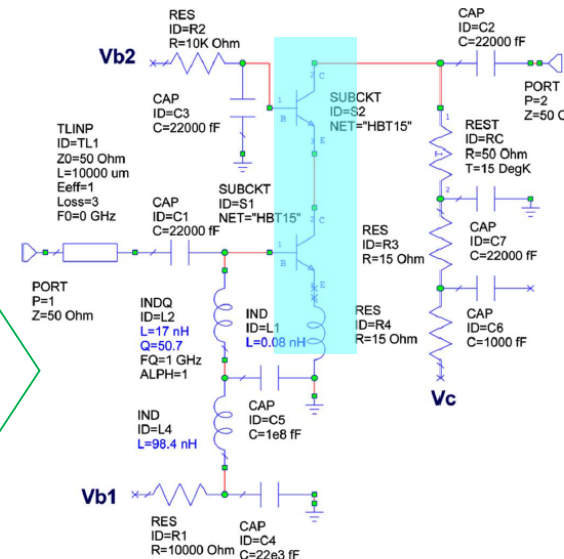
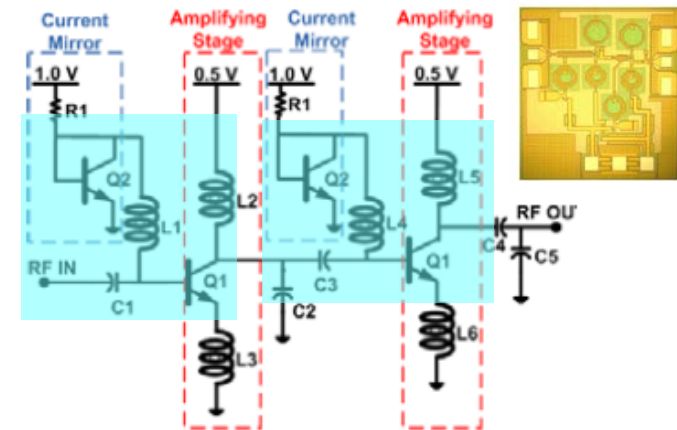


Fig. 12. Schematic of cascode 0.5–3-GHz amplifier modeled with circuit sim-

... frontend for LID: LNA ...noise 20

A question would be: why do not use microwave amplifiers for the readout of dc squid, or, in general, not modulated detector?

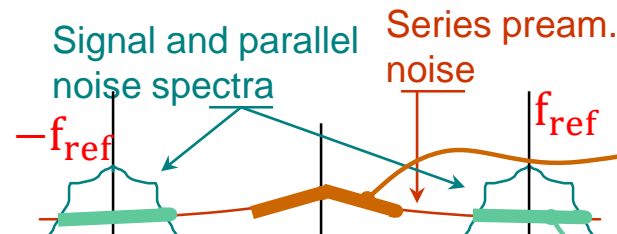
The III-V compounds are heterostructures obtained by melting dissimilar materials together. At their interfaces defects can form which can act as capture centres for charge carriers. Noise effects add if the duration of the signal is comparable to the trapping time constant.

Generation-recombination of carriers at trapping centres gives low-frequency noise that worsens the S / N for dc squid.

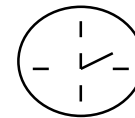
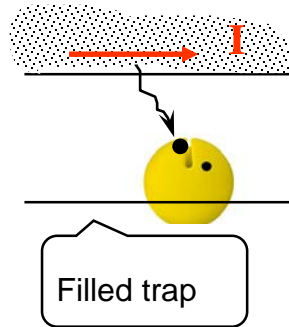
Signal and parallel noise spectra

Series pream. noise

MODULATION

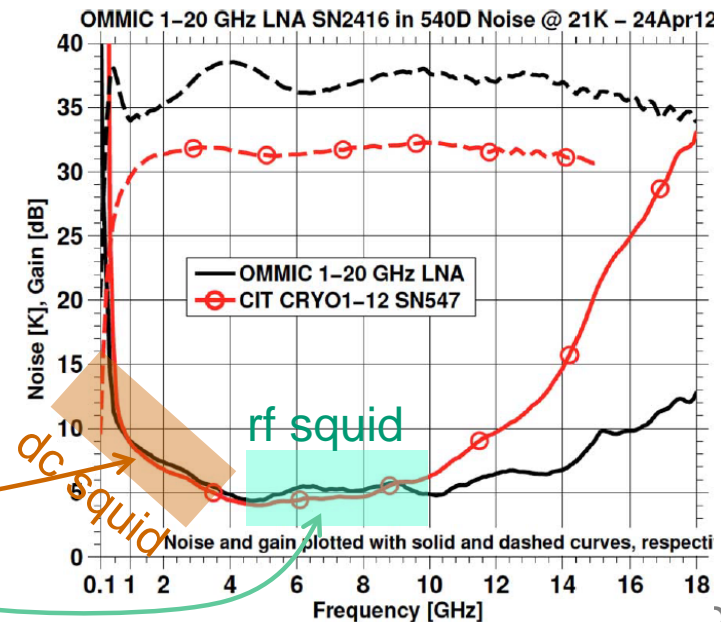
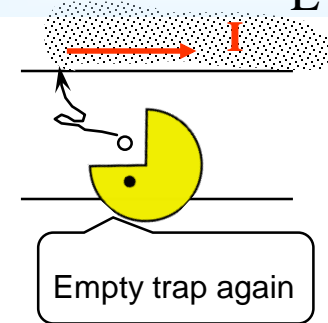


$$I = e(N_{TOT} - 1)\mu \frac{V_{BIAS}}{L^2}$$



$$\Delta t = \tau_0 e^{-t/\tau}$$

$$I = eN_{TOT}\mu \frac{V_{BIAS}}{L^2}$$

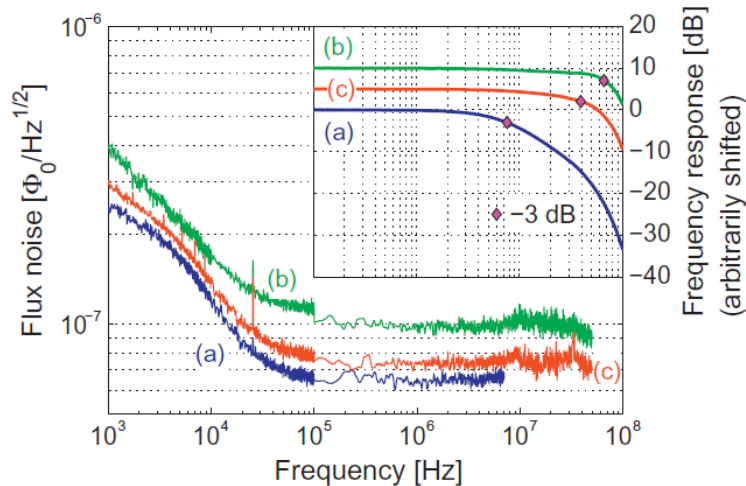


Nevertheless... low frequency noise is not an intrinsic noise source and technological processes could be optimized for low noise. Here we have 2 examples.

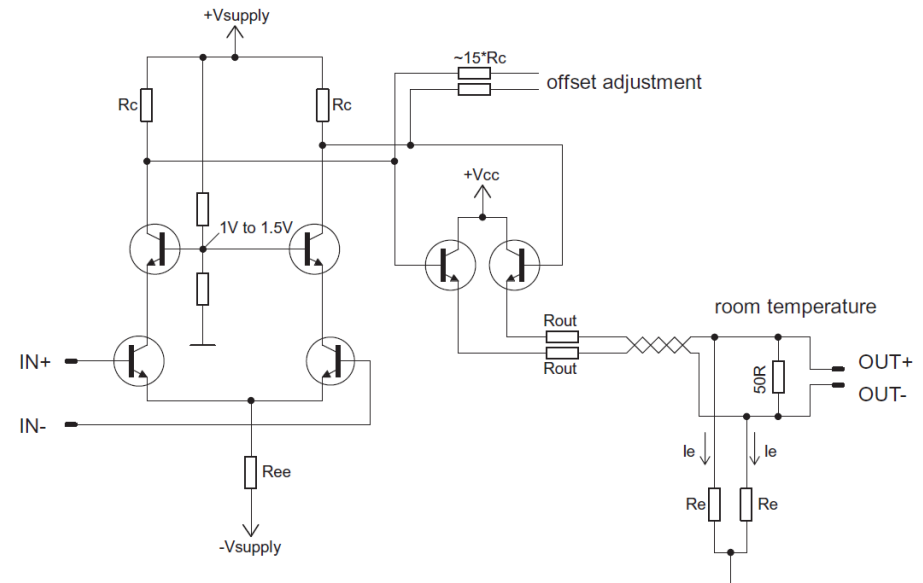
With this cryogenic amplifier in SiGe the noise was very low and authors of the experiment claimed a noise of below $8 \times 10^{-8} \Phi_0/\sqrt{\text{Hz}}$!

The SiGe adopted was the **NESG3031**.

A differential input pair cascoded and buffered in open loop configuration.



NESG3031 SiGe



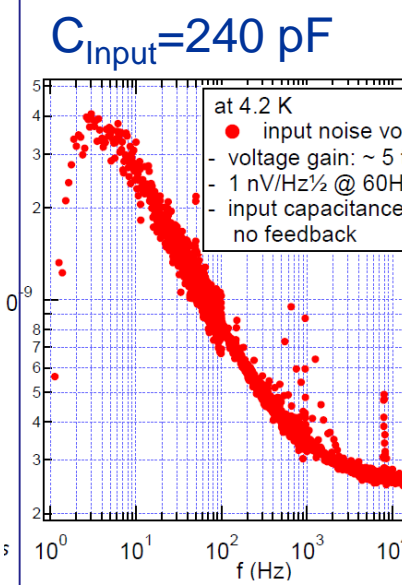
... frontend for LID: LNA ...noise 22

A cryogenic family of HEMT is available from CNRS/C2N.

Best performance is obtained at 4.2 K with the 200pch, having an input capacitance of slightly less than 250 pF.
Noise is around 5 nV/ $\sqrt{\text{Hz}}$ @ 1 Hz and about 0.2 nV/ $\sqrt{\text{Hz}}$ @ 4.2 K.
The HEMT is capable to work up to 1.5 GHz, being optimized for low frequency operation. This result was consequence of a long term search in design, material growth, fabrication process and characterization.

The factor of merit $C_A e_A^2$ for this HEMT family is 3×10^{-27} J, a rather good feature.

To compare: a standard HEMT/Si-MOS device has order of 10^{-23} J, while a good Si JFET operated at room temperature has 2×10^{-29} J.



Name		200pch	100pch	30pch	5pch	1pch
$L_g \times W (\mu m^2)$		1.5×10^5	6.4×10^4	2.0×10^4	2.0×10^3	4.0×10^2
$C_{gs} (pF); C_{gd} (pF)$		236; 8.9	103; 8.9	33; 3.5	4.6; 1.0	1.8; ~0.6
$V_{ds} (mV); I_{ds} (mA)$		100; 1.0	100; 1.0	100; 1.0	100; 1.0	100; 0.5
$g_m (mS); g_d (mS)$		52; 0.4	40; 1.2	115; 1.3	44; 1.3	15; 0.8
$f_t = g_m / (2\pi C_{gs}) (Hz)$		3.5×10^7	6.2×10^7	5.5×10^8	1.5×10^9	1.3×10^9
$e_n (nV/Hz^{1/2})$	@1Hz	5.4	6.3	14	30	100
	@10Hz	1.7	2.1	4.5	12	30
	@100Hz	0.52	0.76	1.5	4.5	10
	@1kHz	0.24	0.34	0.57	1.4	2.7
$e_{n-white} (nV/Hz^{1/2})$						0.4
$i_n (aA/Hz^{1/2})$						3.6
						57
$R_n (\Omega)$						2.8×10^{10}
$T_{nt} (mK)$						3.7×10^7
						13
						5.6

Noise Model of cryogenic High Electron Mobility Transistor, Low threshold and high discrimination Ge cryogenic detector for Coherent Elastic Neutrino Nucleus Scattering and low mass Dark Matter^a (#373)

A. Julliard¹, J. Billard², D. Chazotte¹, J.-B. Filippini¹, D. Mink³, L. Vagneron¹, Q. Dong⁴, A. Cervera⁵, C. Ulysse⁶, Y. Bai⁷, X. de la Broise⁸, A. Boudry⁹, C. Nones¹⁰, A. Phipps¹¹

¹ Univ. Lyon, Université Lyon 1, CNRS/IN2P3, BP 68, F-69622, Villeurbanne, France
² CNRS, CNRS, Univ. Paris-Saclay, Univ. Paris-Saclay, 91120 Palaiseau, France
³ INFN, CNA, Università Paris-Saclay, F-91191 Gif-sur-Yvette, France
⁴ Department of Physics, Stanford University, Stanford, CA 94305, USA

HEMT developed at CNRS/C2N

AlGaAs/GaAs hetero-junction. Energy band diagram. The investigated HEMTs are based on an AlGaAs/GaAs hetero-structure grown by MBE (Molecular Beam Epitaxy). It consists of a GaAs buffer layer, a 20 nm AlGaAs spacer layer (thicker than for commercial HEMT), a Si δ-doping layer, a 15 nm undoped AlGaAs barrier layer, and a 6 nm undoped GaAs cap layer.

$I_{ds}-V_{ds}$ characteristics of a 100 pF C_{gs} HEMT @ 4.2 K

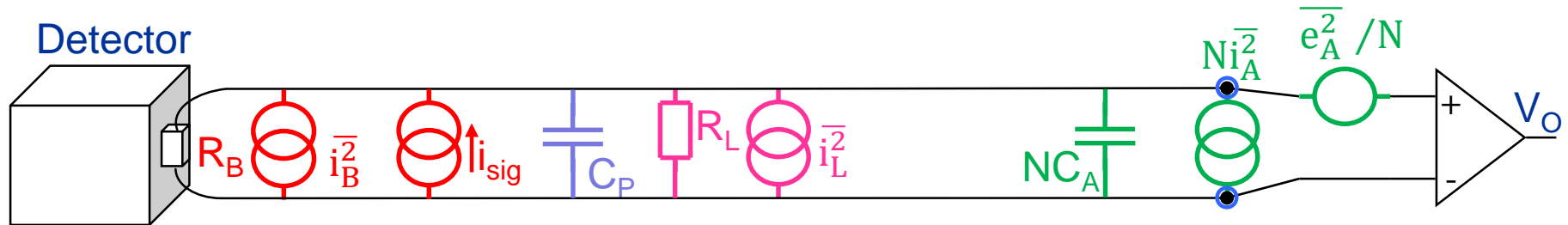
- High transconductance can be obtained with typical power dissipation < 100 μW
- Characteristics unchanged at T < 4K and noise improves a bit
- HEMT can be placed close to the detector: low cabling capacitance

Index: Frontend for Medium and High impedance Cryogenic Detectors, the medium impedance case

- Preamble;
- The base for the choice of the front-end configuration;
- Frontend for Low impedance Cryogenic Detectors;
- Frontend for Medium and High impedance Cryogenic Detectors:
 - Medium impedance detectors

Front-end optimization with medium to large impedance detectors

Coming back to our scheme a last time:



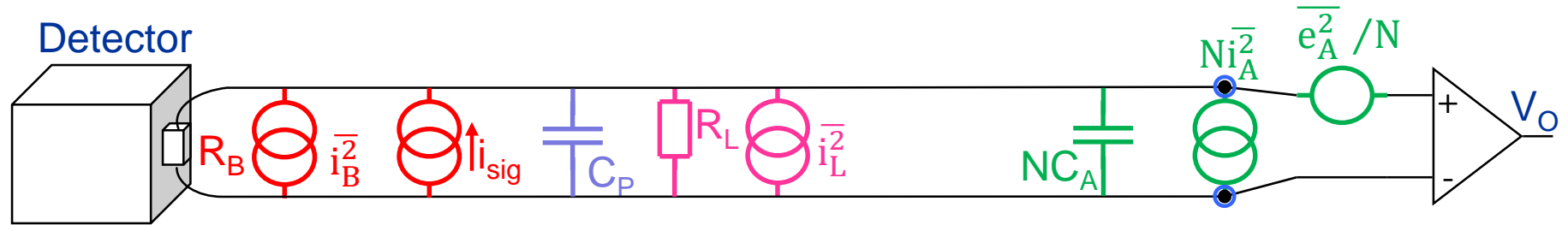
$$\frac{S^2}{N^2} = \int \frac{|V_O(\omega)|^2}{V_O^2(\omega)} df = \int \frac{i_{sig}^2(\omega)}{\frac{1 + \omega^2 (C_P + N C_A)^2 (R_B \parallel R_L)^2}{(R_B \parallel R_L)^2} \frac{e_A^2}{N} + \bar{i}_B^2 + \bar{i}_L^2 + N \bar{i}_A^2} df$$

The medium to large impedance detectors are the field of thermistors as thermal sensors.

The impedance values extend from a few hundred $K\Omega$ to hundreds of $M\Omega$, while the speed of the signals extend from rise time of a few μs to tens of ms , or the signal bandwidth from about one hundred KHz down to tens of Hz .

Also in these cases the front-end works most of cases unmatched and the S/N must be optimized on case-by-case basis.

Front-end optimization with medium impedance detectors



Small crystals need small thermistors. Thermal signal is quite fast and thermistor impedance is maintained small to minimize signal integration from the parasitic and amplifier input capacitance. The range being between hundreds $K\Omega$ to few tens of $M\Omega$.

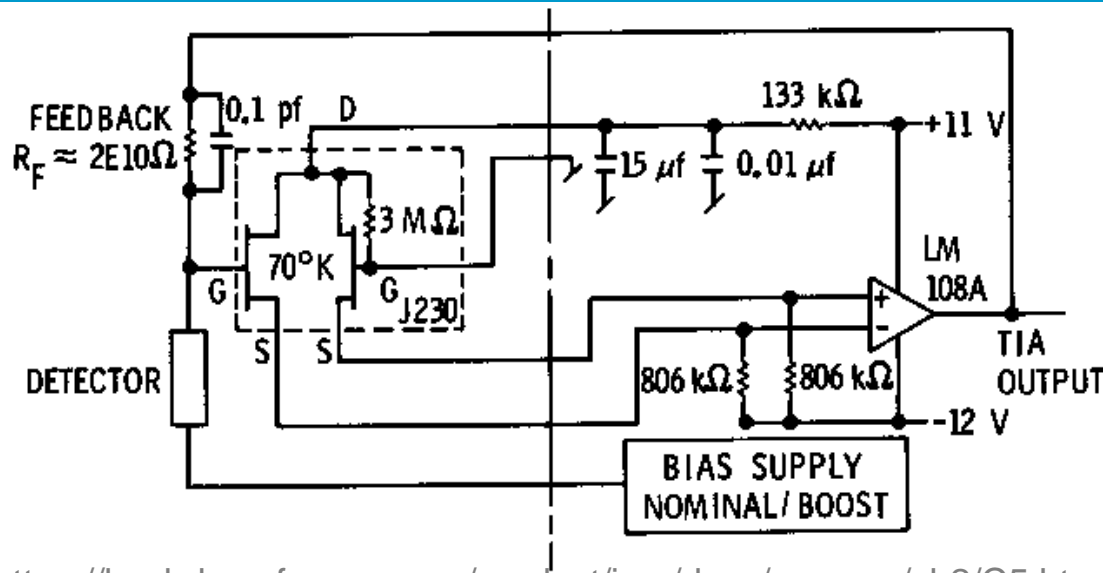
Total capacitance should be less than **10 to 20 pF** to avoid signal integration or amplifier series noise early contribution.

If these constraints are satisfied the S/N is therefore limited by:

$$(i_{sig}(\omega) = \alpha F(\omega) U_{energy}) \quad \frac{S^2}{N^2} \approx \int_{\text{Signal BW}} \frac{\alpha^2 U_{energy}^2 R_B^2}{\overline{e_A^2} + 4K_B T_B R_B + \overline{i_L^2} R_B^2} df$$

... and the constraints are satisfied if the first amplifying stage is cooled....

Front-end optimization with medium impedance detectors 2



According to Dan McCammon the first use of a cryogenic setup was with the IRAS infrared satellite. The readout was for photodetectors.

A pair of source follower Si-JFET were put at cold and a second warm stage implemented a trans-impedance feedback with a feedback resistor of 20 G Ω (Eltec model 102 metal film) held at 2 K.

<https://lambda.gsfc.nasa.gov/product/iras/docs/exp.sup/ch2/C5.html#tabC6> and Proc. SPIE 0445, Instrumentation in Astronomy V, (9 January 1984); doi: 10.1117/12.966154

Each detector is biased through a load resistor of 40 M Ω by a low noise DC voltage supply, adjustable from 0 to 10 volts. The detector voltage is measured through a JFET source follower amplifier (gain ~ 0.995) mounted near the detector but thermally isolated from it. The amplifier uses dual JFETs connected in parallel, and suspended by Kevlar threads inside a copper can, so that the JFET bias power can heat it to an operating temperature of ~ 70 K, similar to that used for the *IRAS* detectors. Each amplifier has its own copper cooling strap directly attached to the instrument mounting flange. Wires into the bolometer housing are filtered against radio and microwave energy by being cast into an iron-loaded epoxy disk. Nevertheless, the detectors were sensitive to radio frequency emitted by the microprocessor clocks (~ 4 MHz), and beat frequency signals between different clocks were seen as excess noise levels at those frequencies despite efforts to provide additional external decoupling. Fortunately, these beat

J.C. Mather, et al, Event: SPIE's 1993
International Symposium on Optics, Imaging, and
Instrumentation, 1993

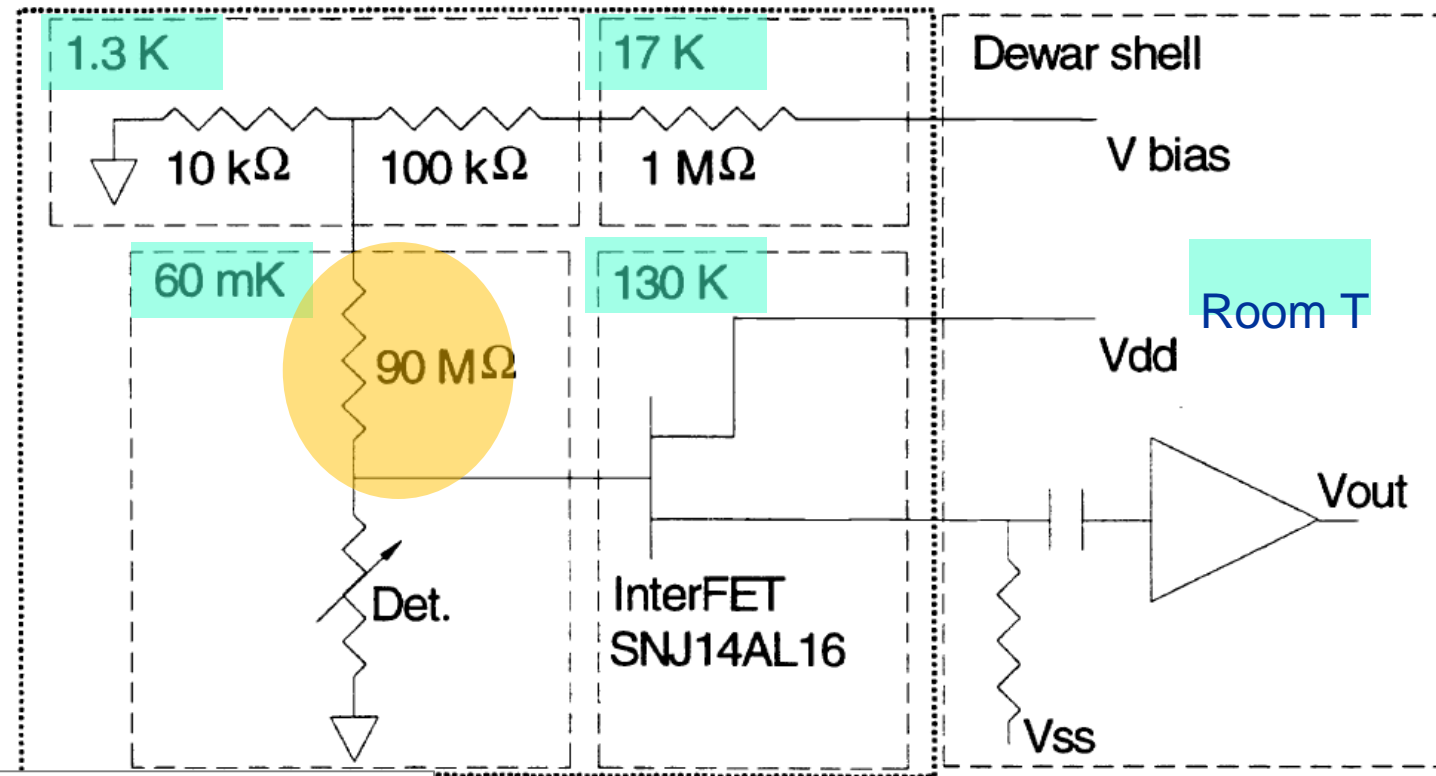
FIRAS was the first spectrometer that used bolometers and the buffered first stage at cold. Interesting: the clock noise was at 4 MHz.

Front-end optimization with medium impedance detectors 3

One of the first following application about the cold readout is this.
A number of considerations are necessary.

The setup is done with the aim of minimizing stray capacitance.

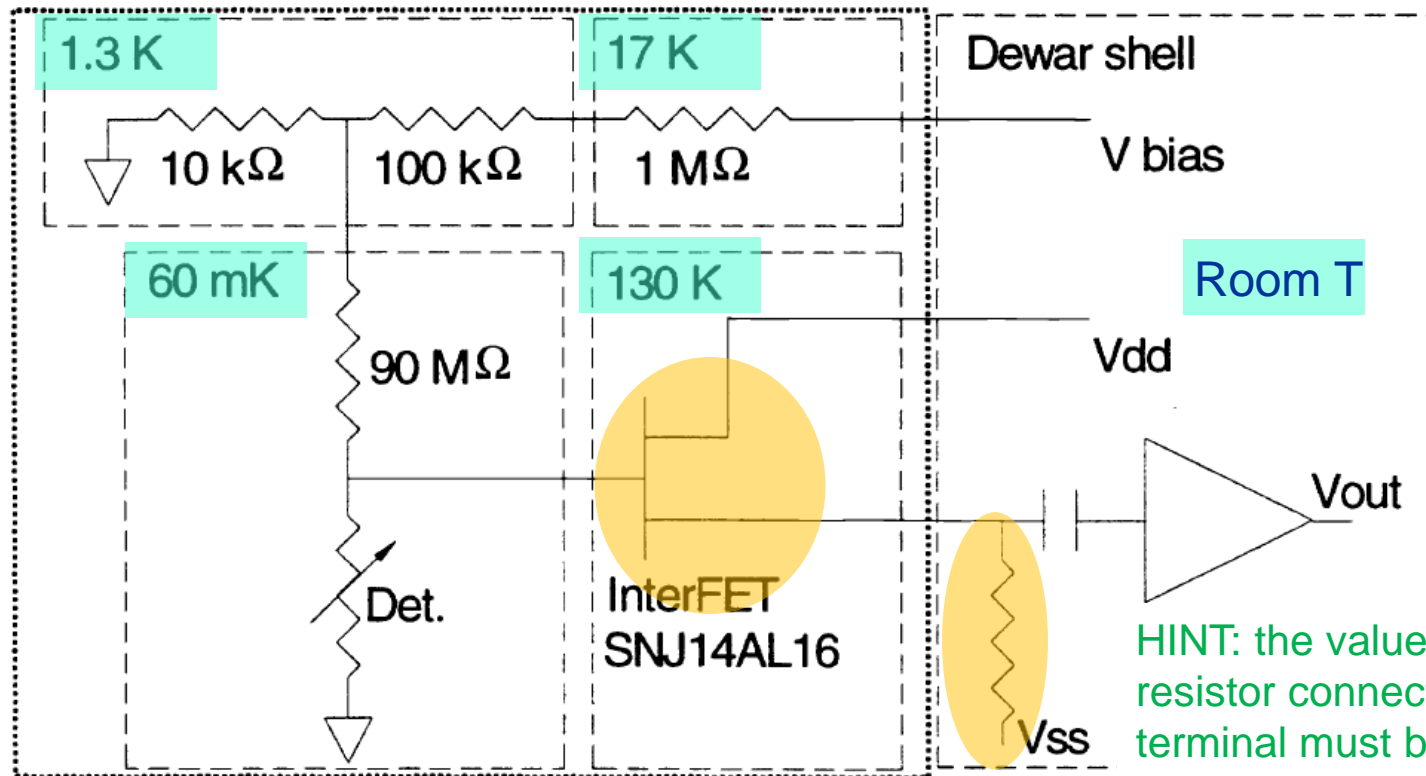
The first step is to locate the load resistor at the same detector temperature: to work at low temperature the load resistor must be made metal film for stability and the value cannot be very large.



This setup was used for readout detector arrays with average resolution better than $5 \text{ eV}_{\text{FWHM}}$ (see ref below).

Front-end optimization with medium impedance detectors 4

The detector signal is slow and III – V compound devices and Si-MOS have low-frequency noise which can be a limit, Si-JFET transistors are more often used at their optimum temperature between 120 K – 150 K. They are normally configured in common-source, unity gain, (to avoid long feedback path from room temperature to inside the fridge) with their biasing resistor at room temperature to minimize power at cold.

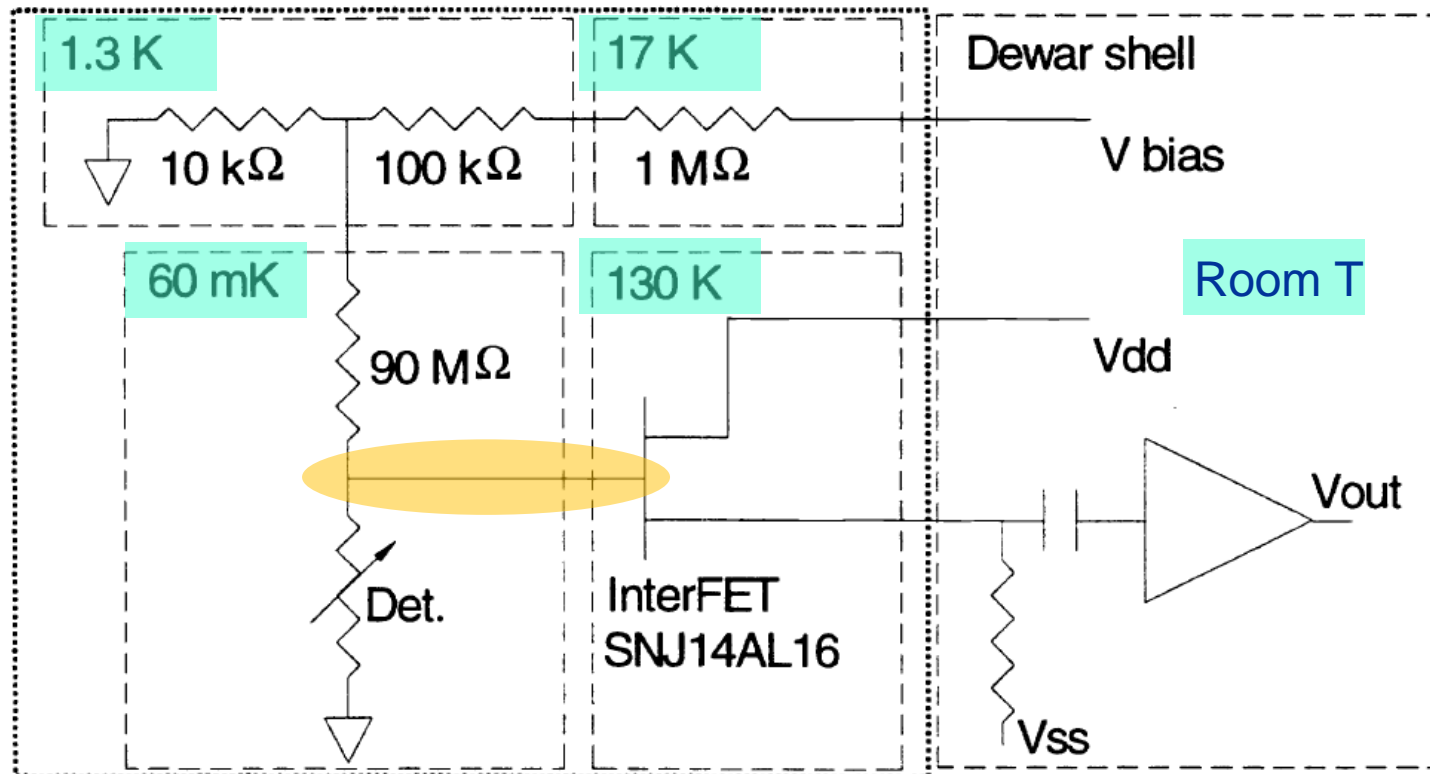


Front-end optimization with medium impedance detectors 5

The connection between the JFET and the detector must be short and the link must assure a negligible heat injection coming from the big thermal gradient.

The JFETs are in a box, suspended with Kevlar cables for example, to minimize thermal conductance toward the bath and create their working environment. Often a heater is put close to them to give an initial increase of temperature, then their dissipation is able to maintain the operating temperature.

The connection to the detector must also minimize microphonic effects.



Front-end optimization with medium impedance detectors 6

Here an example of a very dense link made with superconductive tracks and polyimide to maximize thermal isolation in the readout of a matrix of TES high impedance sensors.



Proc. SPIE 10699, 2018 : doi: 10.1117/12.2312532

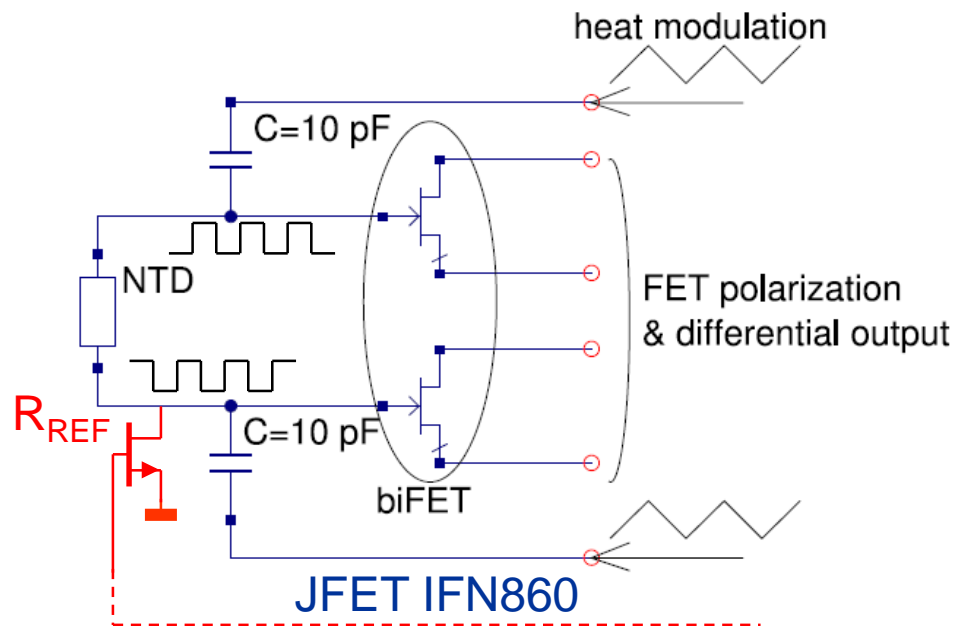
J Low Temp Phys (2018) 193:578–584

LTD-18, gpressina

Front-end optimization with medium impedance detectors 7

EDELWEISS experiment tries to mitigate the low-frequency noise in series to the JFET gate with an AC bias: detector signal modulates the AC bias while the series noise does not, so that its contribution is that at the modulation frequency, where low-frequency noise contribution is negligible.

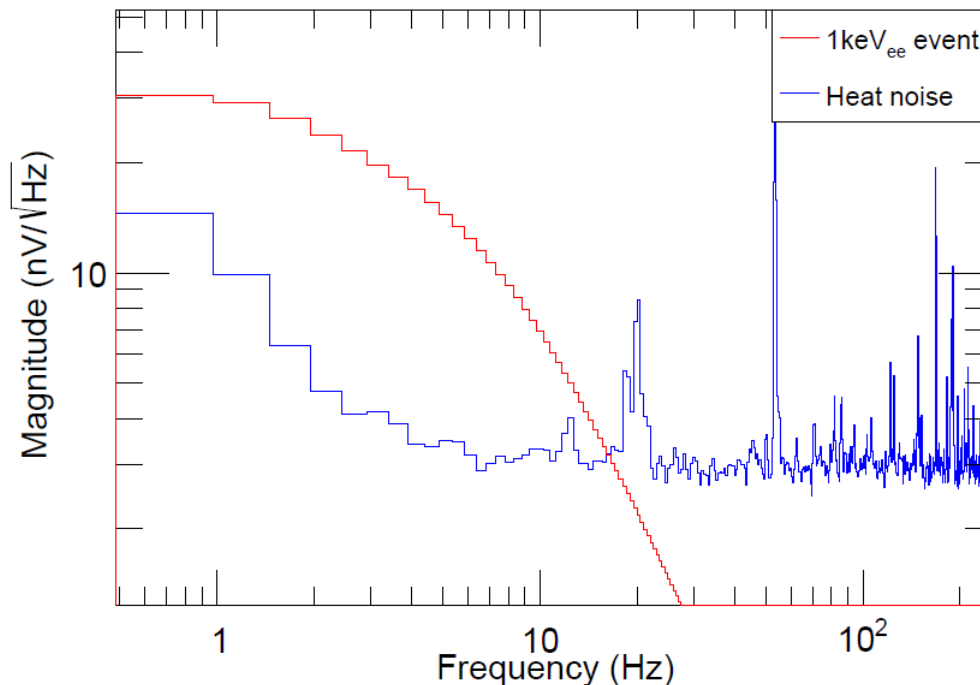
To maintain symmetry the bias is differential given through 2 small capacitances: the AC bias is triangular and integrated across the capacitances in order to become a square signal. This is a quite interesting solution as the detector sees a bias that changes only the sign, but never the power value.



A reference resistor that establishes the gates to ground is necessary, but it does not need to be precise and stable and it can be selected for not affecting the noise. They use a JFET biased in cut-off obtaining a resistance value greater than $10^{12} - 10^{13}\ \Omega$.

Front-end optimization with medium impedance detectors 8

JINST 2017 12 P08010



Noise result is quite good.
The frequency of the bias is between 500 Hz and 1 KHz (I do not know the actual value for this plot).

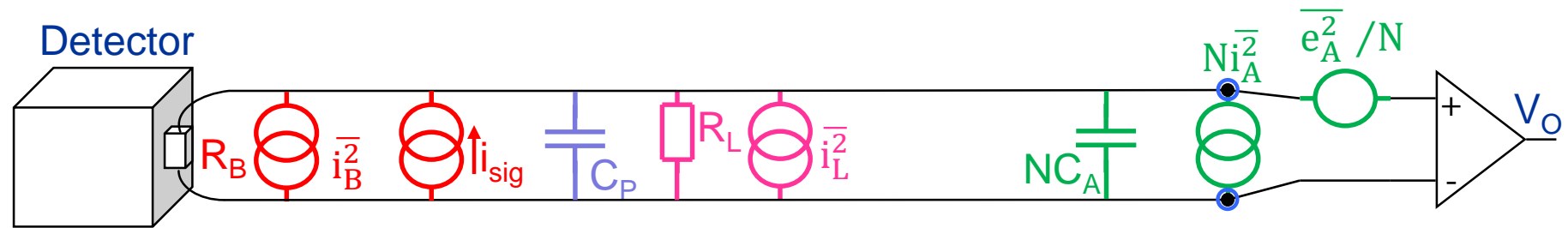
The mitigation of the low frequency noise seems efficient with the spectrum of the signal superimposed for comparison.

Residual low frequency noise could be from detector friction and wire vibration, namely, mechanical microphonism, parallel noise, the actual effect limiting the final resolution in several applications.

Index: Frontend for Medium and High impedance Cryogenic Detectors, the high impedance case

- Preamble;
- The base for the choice of the front-end configuration;
- Frontend for Low impedance Cryogenic Detectors;
- Frontend for Medium and High impedance Cryogenic Detectors:.
 - High impedance detectors

Front-end optimization with high impedance detectors 1



$$(i_{\text{sig}}(\omega) = \alpha F(\omega) U_{\text{energy}}) \quad \frac{S^2}{N^2} \approx \int_{\text{Sig.BW} \cap \text{parasitic}} \frac{\alpha^2 U_{\text{energy}}^2}{\omega^2 (C_P + N C_A)^2 \left(\frac{e_A^2}{N} + i_B^2 + i_L^2 + N i_A^2 \right)} df$$

We speak about thermistor impedance close or in excess of hundred MΩ.

In these cases is almost impossible to try to match the front-end to the detector.

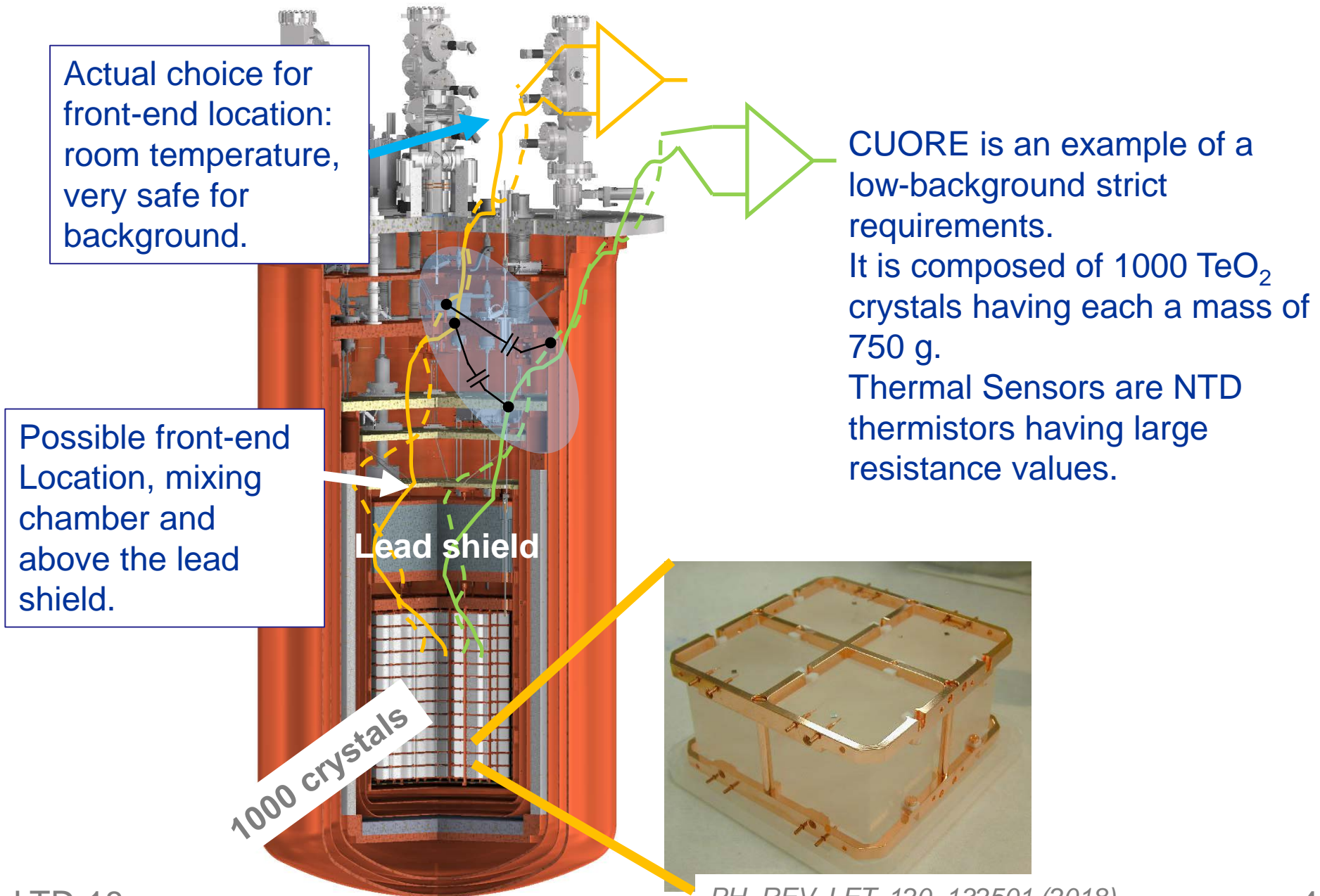
Signal bandwidth and parasitic capacitance are very important for defining which parameters to optimize for the front-end.

Front-end optimization with high impedance detectors 2

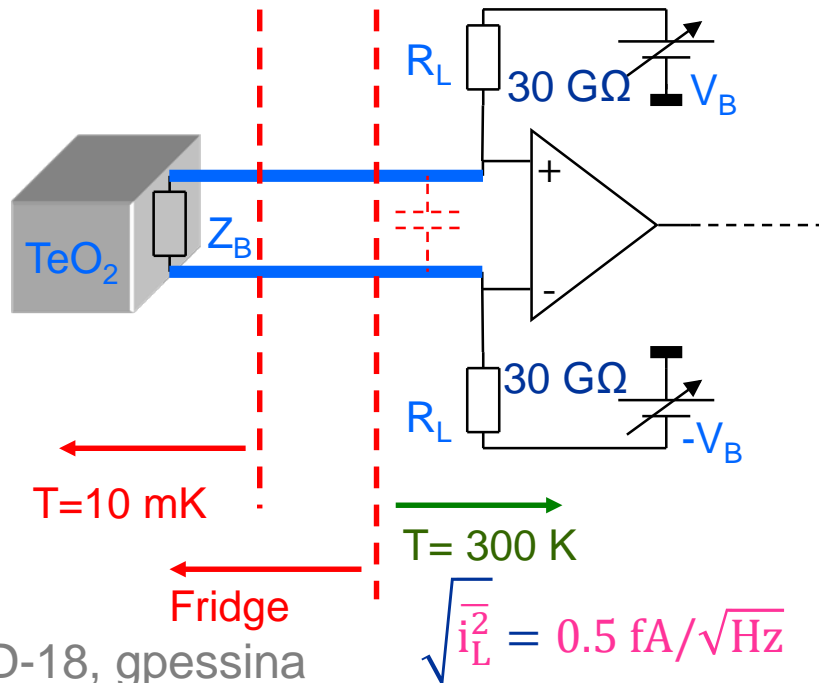
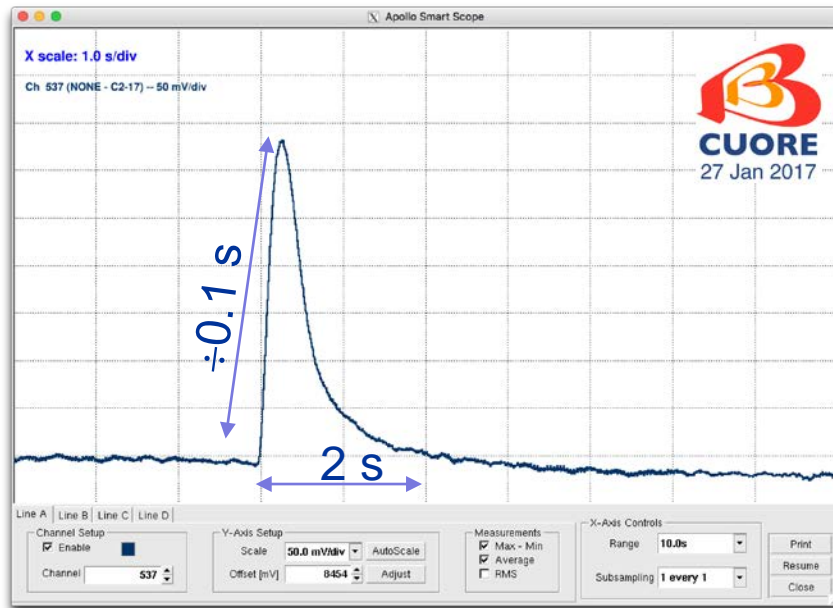
The reasons for large impedances and large capacitances are several:

- ✓ A very large dynamic range of signals, typical of neutrino physics, which extends from a few KeV up to a few tens of MeV asks for thermistors that can handle large voltages;
- ✓ Low background, if required, finds benefit if the front-end is operated far from the detector;
- ✓ The detector is composed of a large-mass crystal to which the thermistor is glued: to reduce its thermal capacity to a minimum, the temperature must be as small as possible, less than 10 mK;
- ✓ Crystals are large and several: heat injection must be minimized;
- ✓ ...

Front-end optimization with high impedance detectors 3



Front-end optimization with high impedance detectors 4

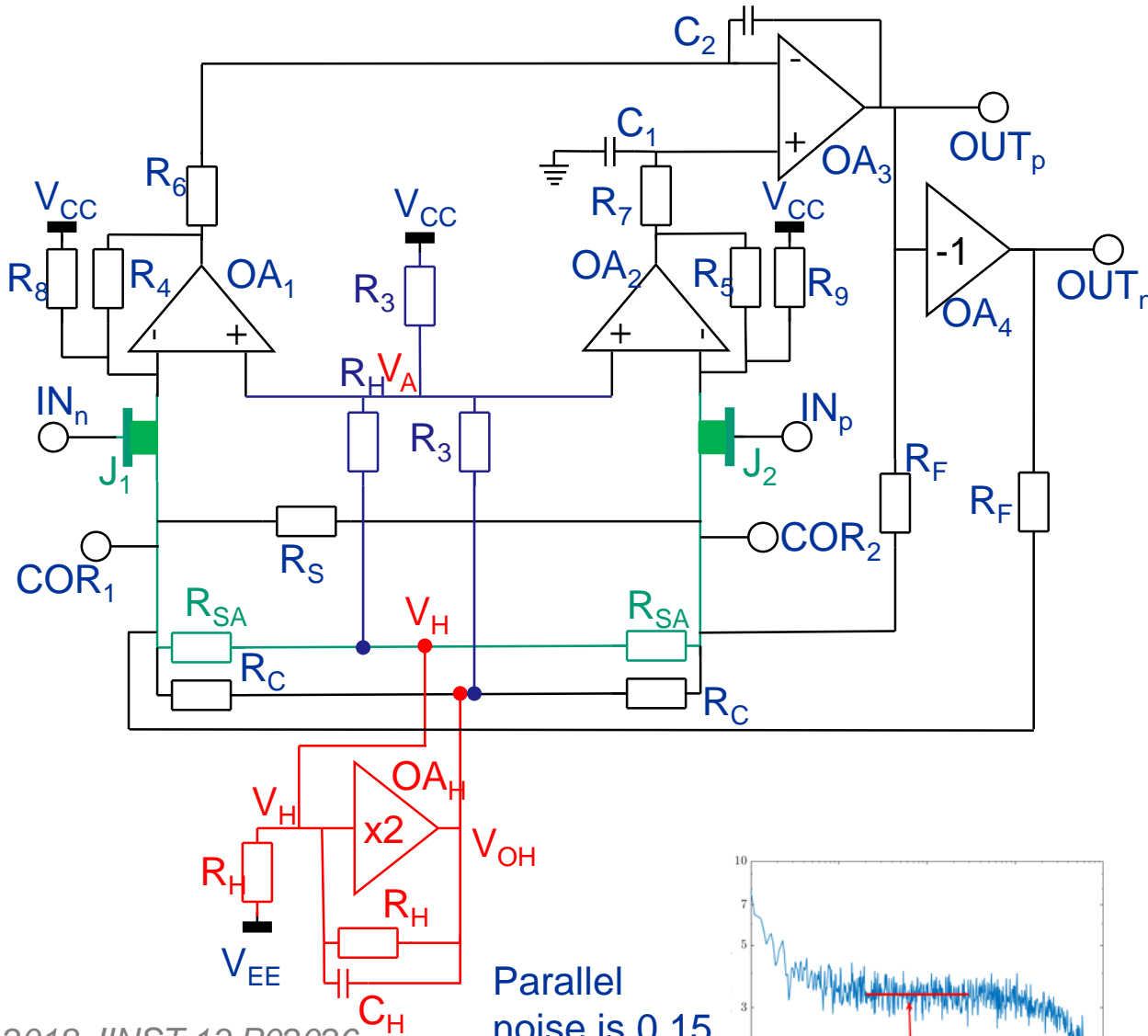


For the sake of background everything in CUORE is macroscopic:

- ✓ Signal BW is less than 5 Hz;
- ✓ Thermistor impedances are a few hundreds M Ω on average;
- ✓ Load resistors at room Temperature are 60 G Ω to minimize their parallel noise;
- ✓ The input capacitance is about 500 pF;
- ✓ Very tight stability of the front-end baseline

$$\frac{S^2}{N^2} \approx \int_{\text{Sig.BW} \cap \text{parasitic}} \frac{\alpha^2 U_{\text{energy}}^2}{\overline{i_B^2} + \overline{i_L^2} + \overline{N_{i_A}^2}} df$$

Front-end optimization with high impedance detectors 5



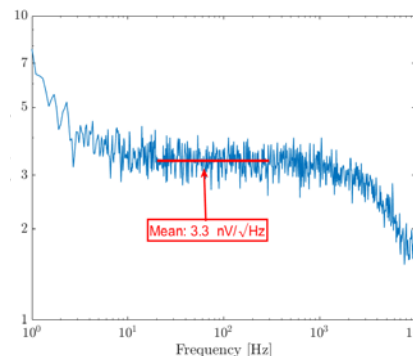
An example of preamplifier operated at room temperature is this: the configuration is instrumentation-differential (with large input impedance) with only 2 JFETs, J₁ and J₂, at the input.

Circuit is designed for having a large open loop gain (extensive use of OpAmp), to obtain a very precise large closed loop gain, and to constraint the JFETs to work at constant current and constant voltage.

The circuit is thermally compensated with a drift smaller than 1 $\mu\text{V}/^\circ\text{C}$.

2018 JINST 13 P02026

Parallel noise is 0.15 fA/ $\sqrt{\text{Hz}}$



Front-end optimization with ionization detectors 1

Before entering into the discussion it is interesting a short historical digression about the origin of the very front-end for particle detectors. Apparently, this has not much to do with the subject of this slides, but ...

What triggered me was a first paper I found that dated 1956: it was the first **voltage preamplifier for particle detectors**, I suppose. It employed valves!

The author of the circuit was **Emilio Gatti** (passed away a few years ago) et Al.

Il nuovo cimento V 3 p 473 1956

The circuit and ...

Look at the supply voltage:
300 V!

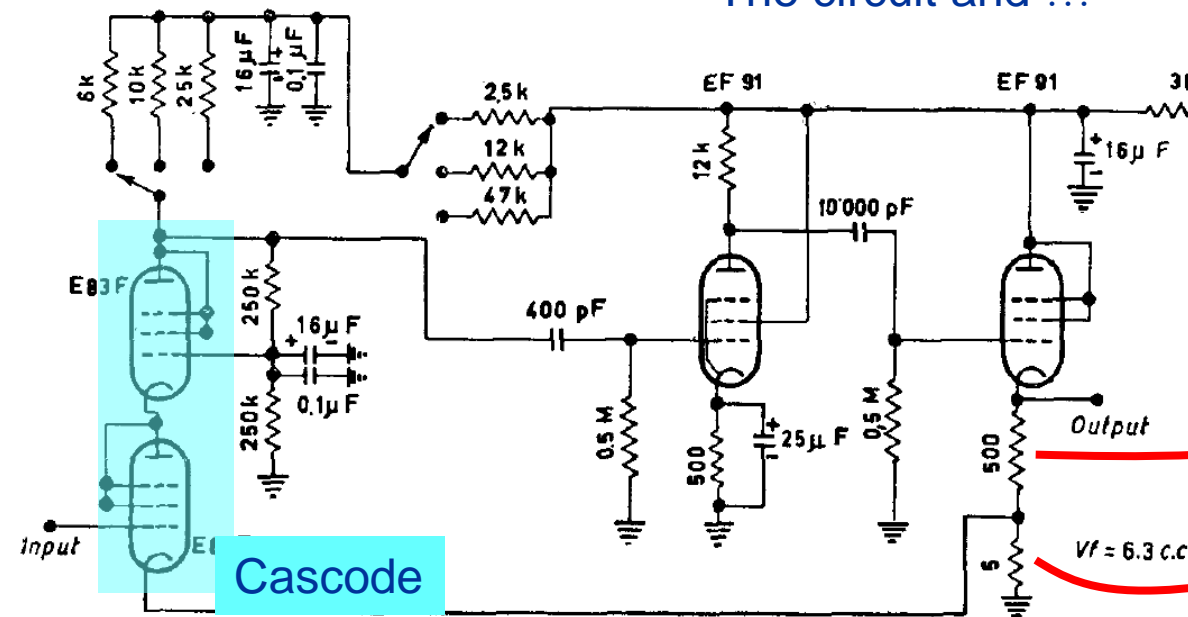


Fig. 3. - Preamplifier scheme.

...the configuration

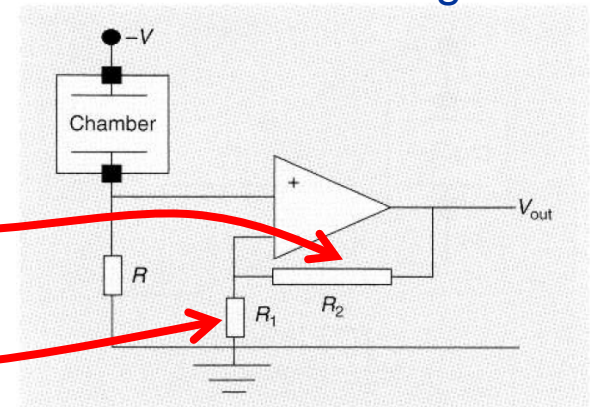


FIGURE 1: Voltage-sensitive preamplifier connected to a gas-filled ionization chamber.

Front-end optimization with ionization detectors 2

Then... I asked **Pier Franco Manfredi** (also passed away) about the first charge sensitive preamplifier. He told me that **Veljko Radeka** was the first to develop a genuine charge sensitive preamplifier.

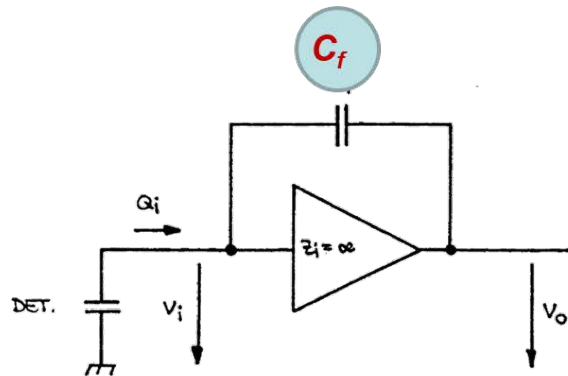
Then I asked to Veljko, which sent me a very nice short report.

The first record of a Charge-Sensitive Amplifier Circuit

1948

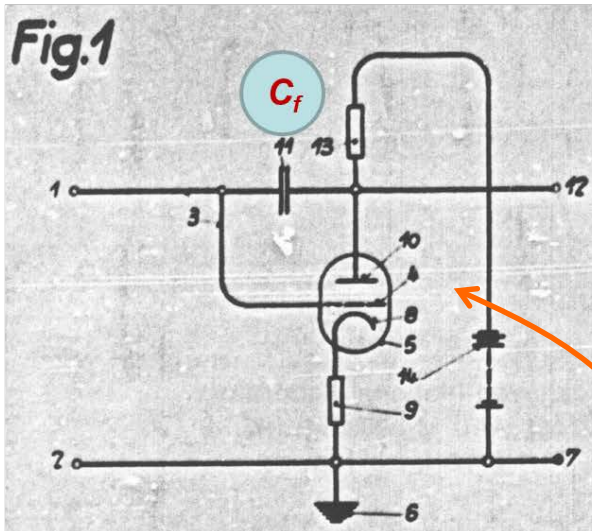


Classical “integrator” known from WWII (1941-5,) appears as charge amplifier in ~1950-ies (Gatti, et al.):



Input capacitance \sim open-loop gain $\times C_f$

Vacuum tube at the input until ~1963 when the first *JFET* is used ...



This configuration is equivalent to a “common source topology”.

Veljko mail:

“The first concept of charge to voltage conversion on a capacitor in feedback appeared in 1948 in a Swiss patent, slide 1; Only one vacuum tube was needed! “

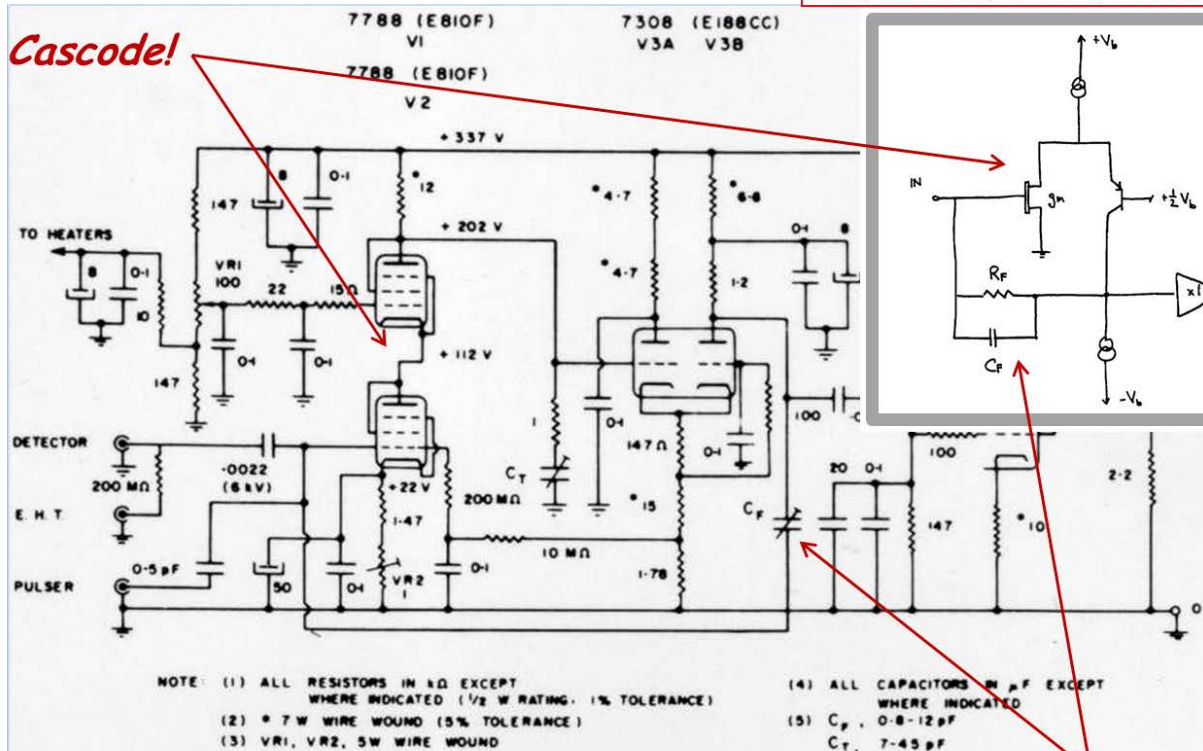
Front-end optimization with ionization detectors 3

According to Veljko, charge sensitive preamplifier for nuclear detector having valves as active components have been used and known since World War III!

The "last word" from vacuum tubes - introducing Ge detectors (Tavendale, 1963)

Original charge preamp with JFET, 1968

The Cascode!



Noise: ~ 200 e rms at 20pF, 1-2 μ s

Feedback

Fig. 4—Charge-sensitive low-noise preamplifier circuit.

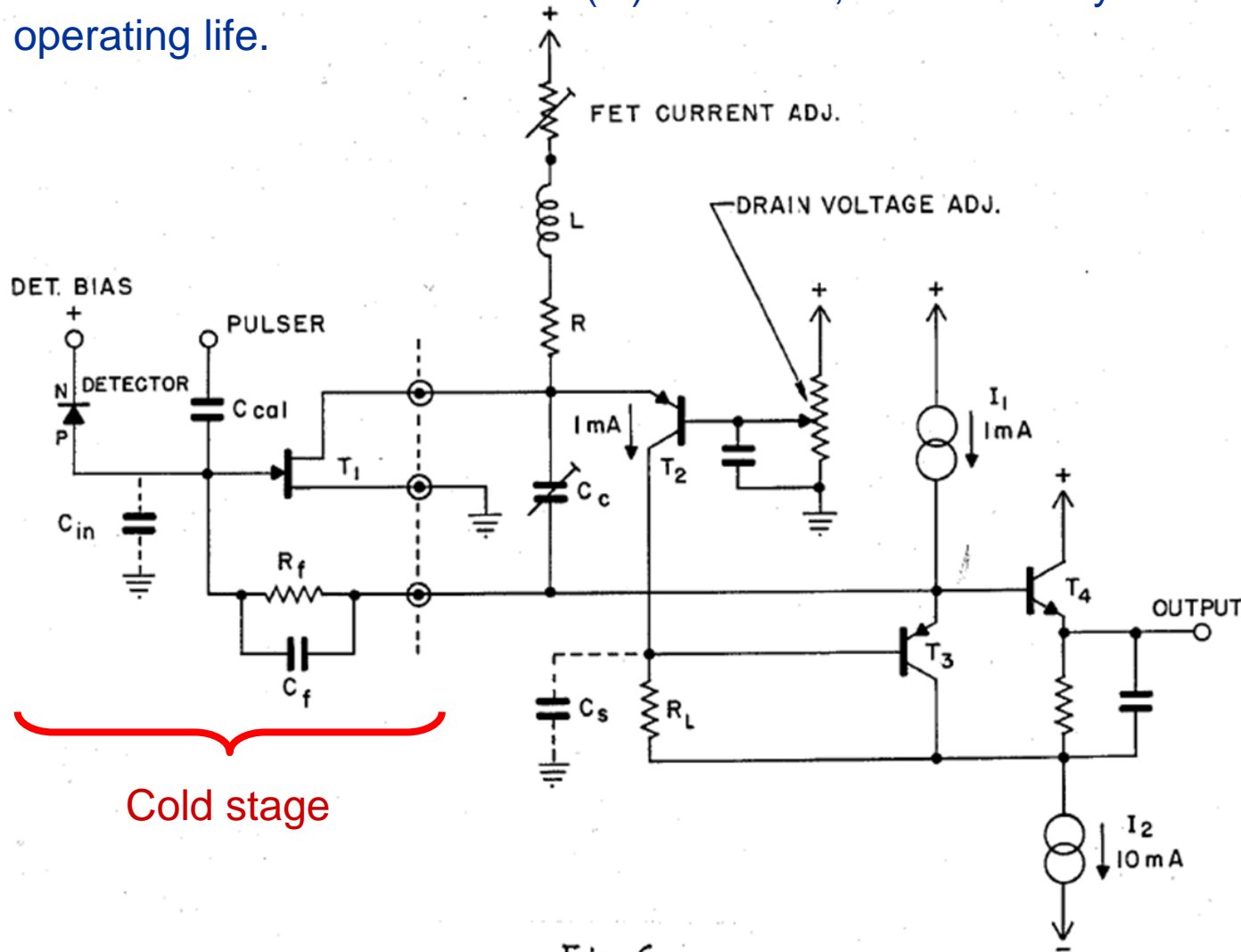
Veljko mail:

“Vacuum tube charge amplifiers were used until ~ 1965 ; an example is shown in slide 2; Cascode configuration with tubes was known from World War II”

Front-end optimization with ionization detectors 4

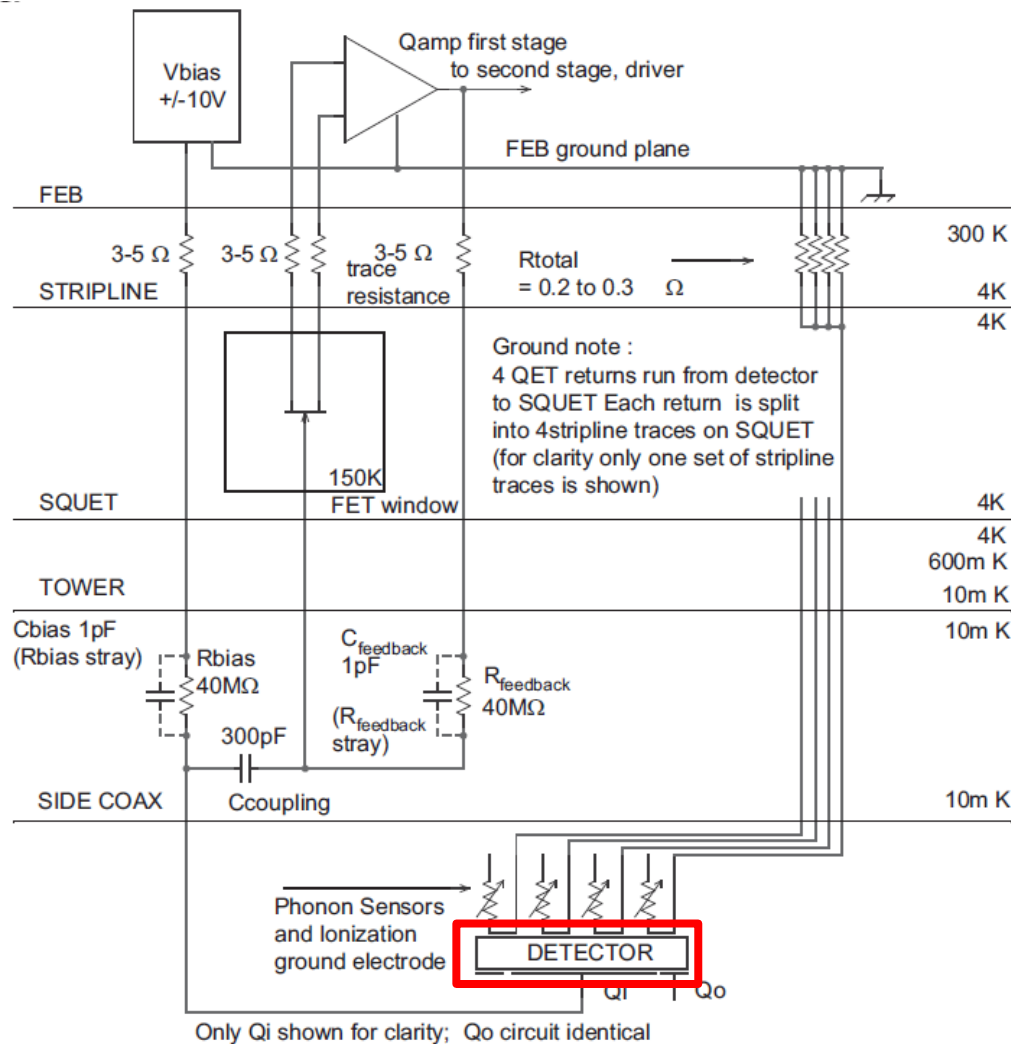
Here is the first charge sensitive preamplifier based on the use of transistors. It was 1968.

This preamplifier is, at the same time, the first example of cryogenic electronic. It was intended for the readout of Ge(Li) detectors, forced to stay at cold during their whole operating life.



Veljko mail:
“In 1968 (paper you requested) I described in some detail, a charge amplifier for germanium detectors, with a JFET at low temperature, slide 3;”

Front-end optimization with ionization detectors 5



Ionization detectors working at deep cryogenic temperatures are readout with a charge sensitive preamplifier, too. The only concern is that the distance of the first stage of the front-end cannot be too close to the detector for avoiding heat injection: the input capacitance is large.

The detector is a very large impedance and microphonism is a concern. In this solution the JFET is biased such a way its gate is close to zero voltage in order to minimize charge injection from parasitic capacitance.

Feedback and bias resistors are 40 M Ω , but located at 10 mK.

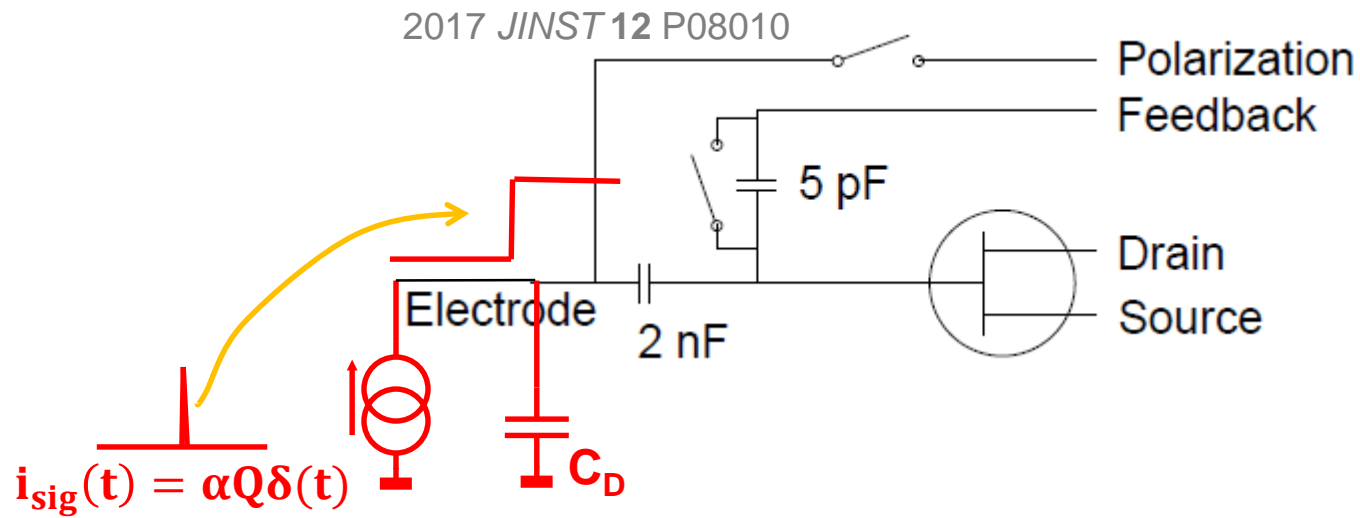
NIMA 591 (2008) 476–489

Front-end optimization with ionization detectors 6

EDELWEISS uses a different approach..

Bias and feedback resistors are replaced with relays which are closed from time to time, tens of seconds scale, to adjust detector bias and the gate of the JFET.

The preamplifier is operated in voltage sensitive configuration, namely, the JFET is a follower, and the charge signal is integrated across the detector, stray and JFET capacitance, about 250 pF.



Front-end optimization with ionization detectors 7

To this we can give a mathematical interpretation:

$$\frac{S^2}{N^2} = \frac{Q^2}{\overline{i_B^2} + N\overline{i_A^2}} \int \frac{\alpha^2}{\omega^2(C_P + NC_A)^2 \frac{\overline{e_A^2}/N}{\overline{i_B^2} + N\overline{i_A^2}} + 1} df = \frac{Q^2}{\overline{i_B^2} + N\overline{i_A^2}} \int \frac{\alpha^2}{\omega^2\tau^2 + 1} df$$

With:

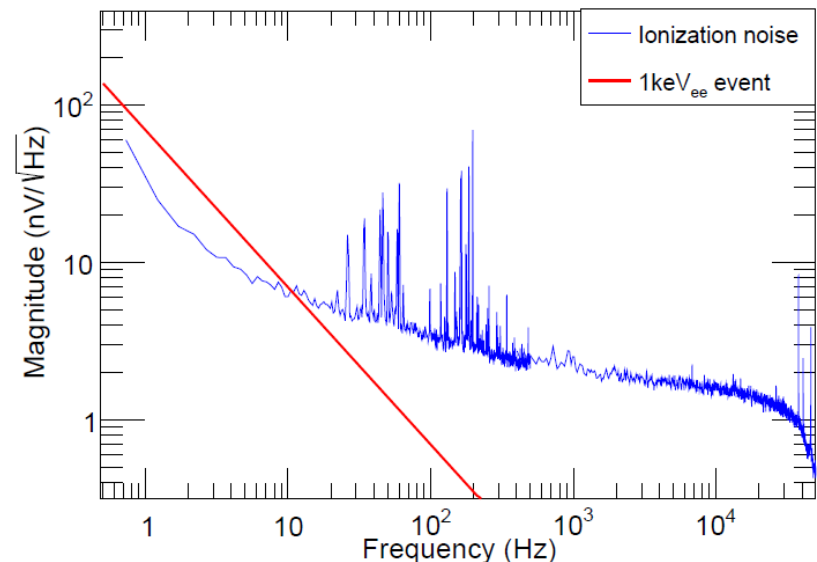
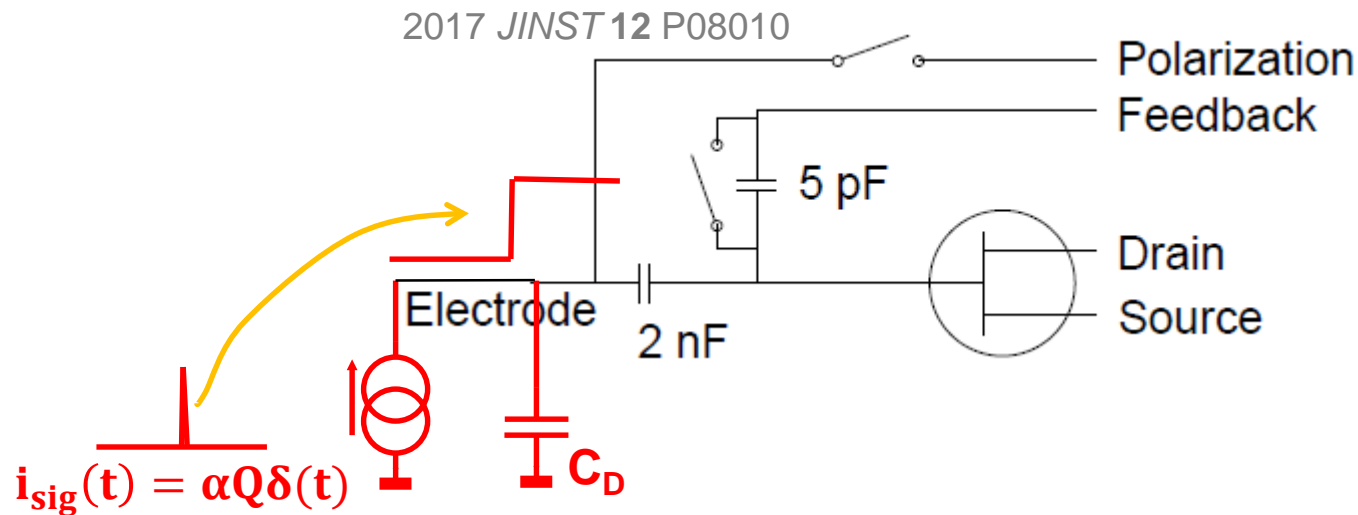
$$\tau = (C_P + NC_A)R_N \quad R_N = \sqrt{\frac{\overline{e_A^2}/N}{\overline{i_B^2} + N\overline{i_A^2}}} \quad \left(\frac{S^2}{N^2} = \frac{Q^2}{2\sqrt{\overline{e_A^2}/N (\overline{i_B^2} + N\overline{i_A^2})}} \right)$$

To summarize:

- ✓ The filter behaves like a low pass filter;
- ✓ If the parallel noise is small, R_N results large and the filtering frequency very small, or the time constant τ , very large (*example R_N is about 120 MΩ when $\sqrt{\overline{e_A^2}} \approx 2 \text{ nV}/\sqrt{\text{Hz}}$, and the gate current 1 fA, with $\tau \approx 10 \text{ ms}$ if the total capacitance is 100 pF*);
- ✓ If the expected signal rate is low, then integration of signal on a very long time makes the noise independent from the preamplifier series noise.

Front-end optimization with ionization detectors 8

The residual frequency dependent noise is mainly (I suppose...) microphonism and the resolution they claim is better than $700 \text{ eV}_{\text{FWHM}}$.

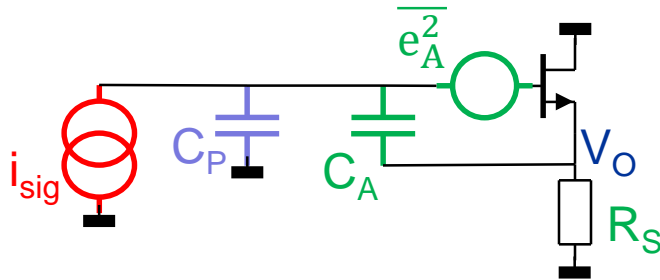


Thank you and sorry for any possible lack ...

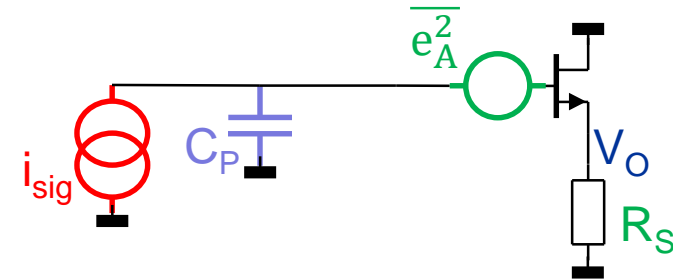
SPARE SLIDES

...noise sources vs configuration

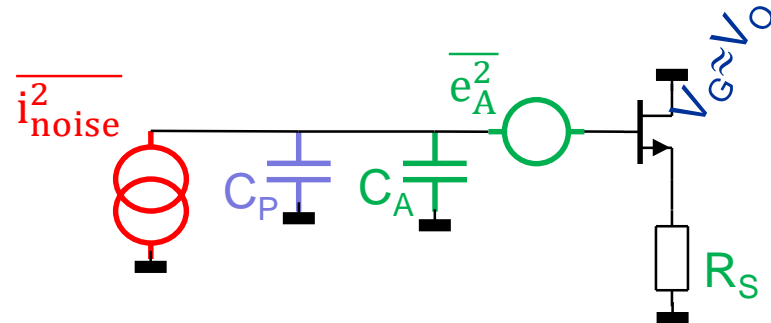
A typical error is to consider this simple and typical configuration:



Equivalent to this, since C_A is bootstrapped:

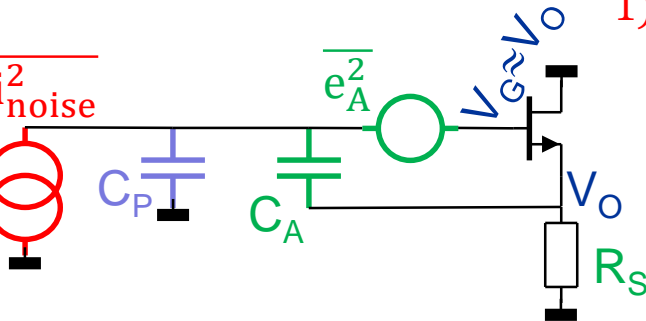


Actually it is equivalent to this, till large frequency:



$$\overline{V_O^2} = \overline{e_A^2} + \frac{\overline{i_{noise_equi}^2}}{\omega^2(C_P + C_A)^2}$$

Proof:



$$1) \text{ If } i_{noise} = 0, \text{ then: } V_O = \frac{C_A}{C_A + C_P} V_O + e_A \Rightarrow \overline{V_{OA}^2} = \left(\frac{C_A + C_P}{C_P} \right)^2 \overline{e_A^2}$$

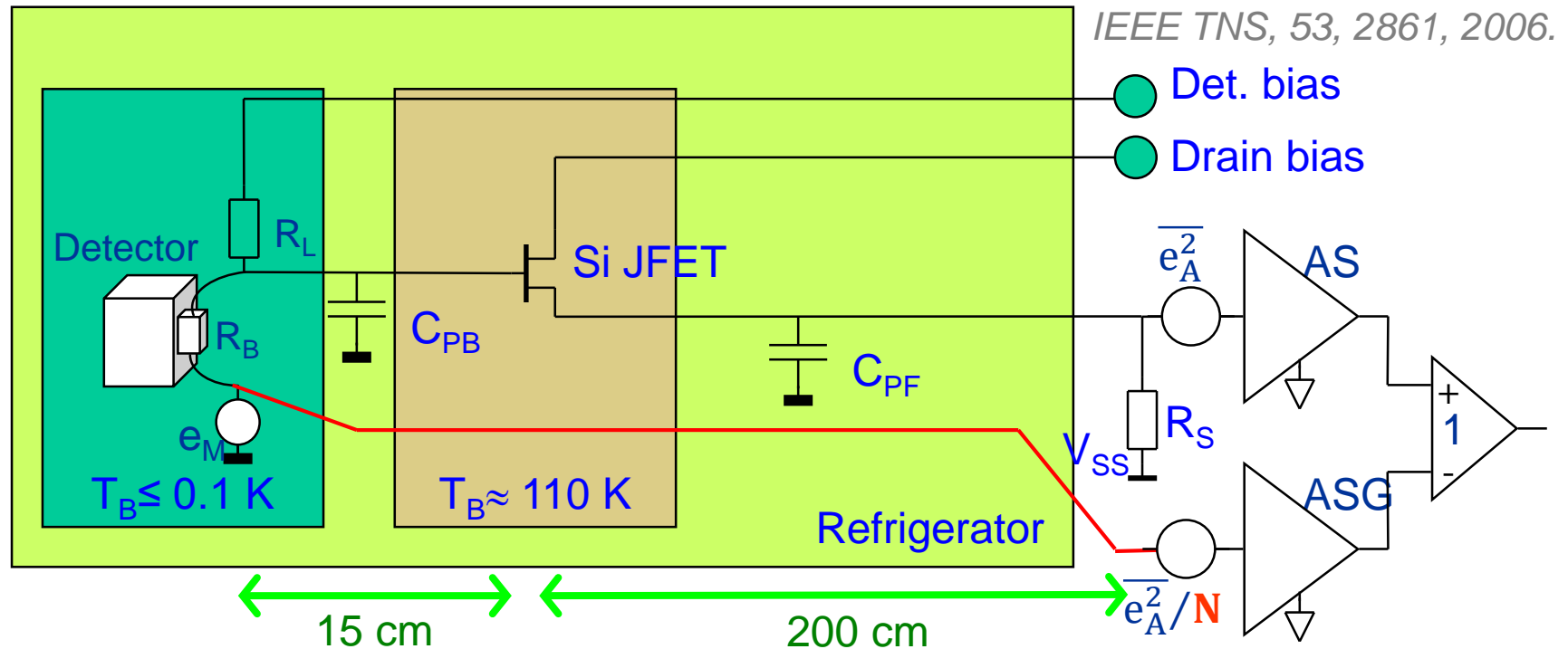
$$2) \text{ If } e_A = 0, \text{ then: } V_O = \frac{i_{noise}}{j\omega C_P} \Rightarrow \overline{V_{OS}^2} = \frac{\overline{i_{noise}^2}}{\omega^2 C_P^2}$$

$$3) \quad \overline{V_O^2} = \left(\frac{C_A + C_P}{C_P} \right)^2 \left[\overline{e_A^2} + \frac{i_{noise}^2}{\omega^2 (C_P + C_A)^2} \right] !!!$$

Front-end optimization with medium impedance detectors

EMI interferences, ground loops, ... can add disturbances and this is often the case when the grounds inside and outside the fridge are different.

To mitigate the noise the difference between the cold stage output and the cold ground node helps.



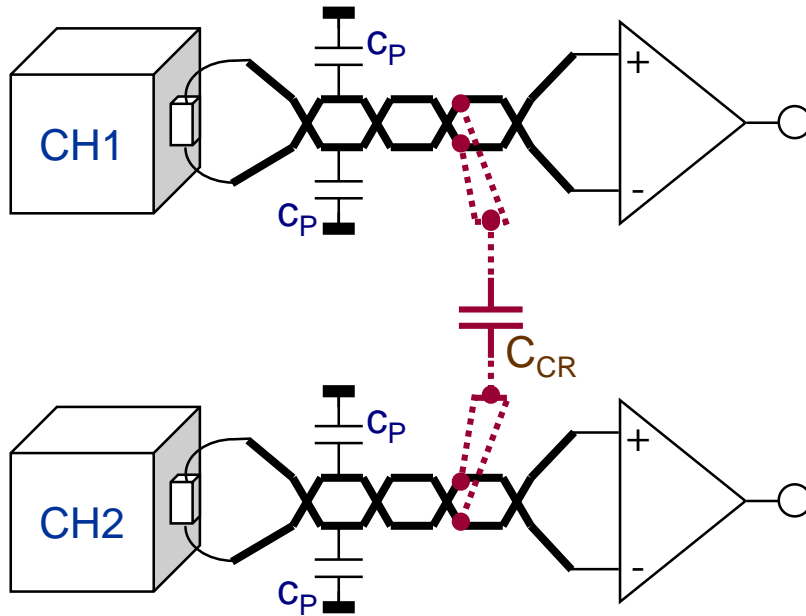
The noise of the second stage is larger if a differential amplifier is used. A possible way to minimize this is to implement the amplifier branch of the reading ground with a very large transistor area, since Ground is a low impedance node.

This amplifier output can be shared by several channels.

Front-end optimization with medium impedance detectors

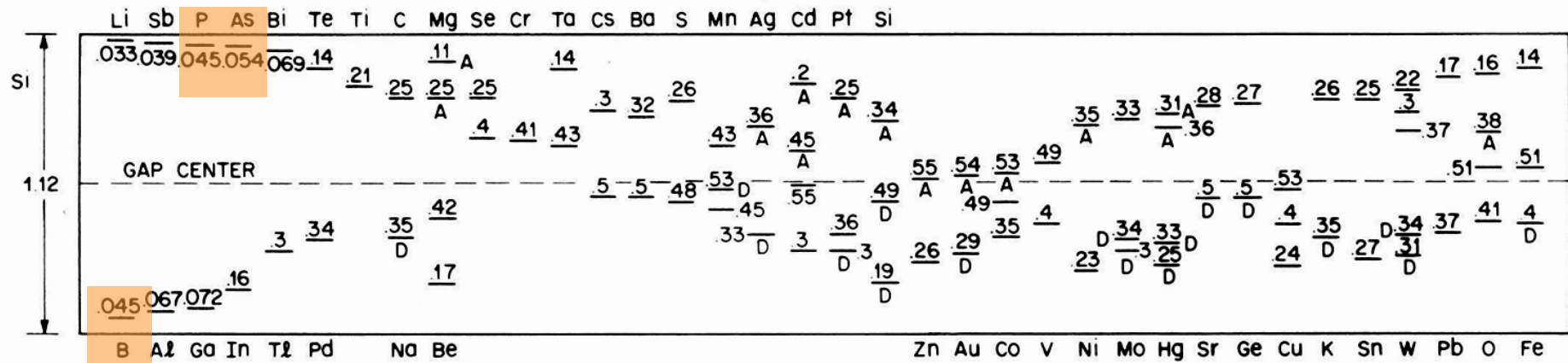
Another source of disturbances arises from the close packaging of channels in an array and when the distance of the front-end from the detectors is not very short: cross-talk.

If the readout is voltage sensitive one efficient way to minimize cross-talk is with the differential configuration, although the larger noise of the preamplifier (coaxial cables can be used, taking care of thermal conductance).



The differential configuration has benefits also in suppressing the so called common mode disturbances, which take advantages from the link length, such as EMI.

Technology 1

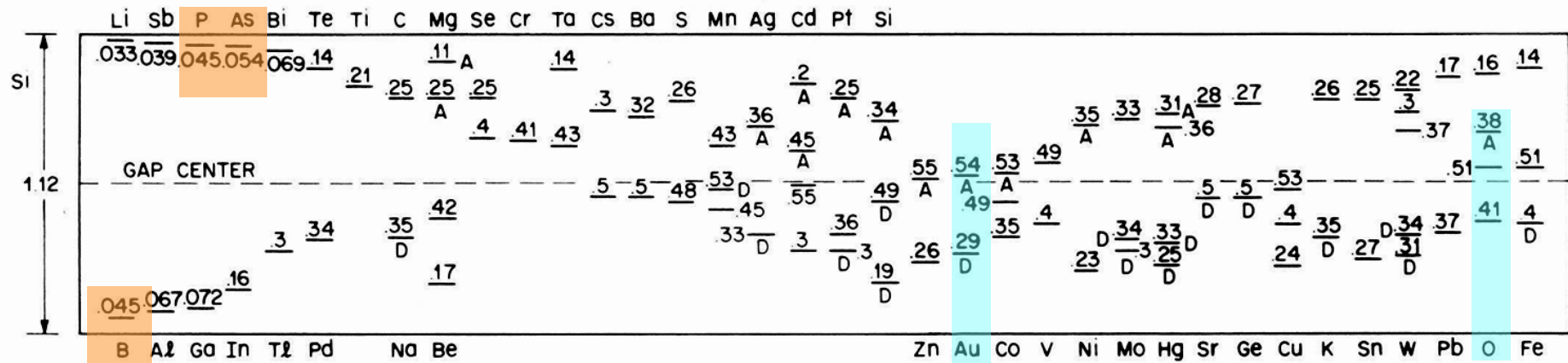


= standard dopants, fast fast centers at room T

Here we have the map of the donor/acceptor atoms in Si.

The energies of the donors/acceptors are distributed in the gap. What does it mean?

Technology 2



= standard dopants, fast fast centers at room T

= most efficient trapping centers at room T

But, why we consider and are interested to all these dopants?

Well, the probability that a carrier falls (is trapped) or escapes (is de-trapped) from a centre is dependent on temperature. The larger is the temperature, the larger is the probability that a deep trap, namely a trap with energy close to the middle of the gap, is active in this mechanism.

Expressed in the other way, the time a trapping centre stays full/empty depends on temperature.

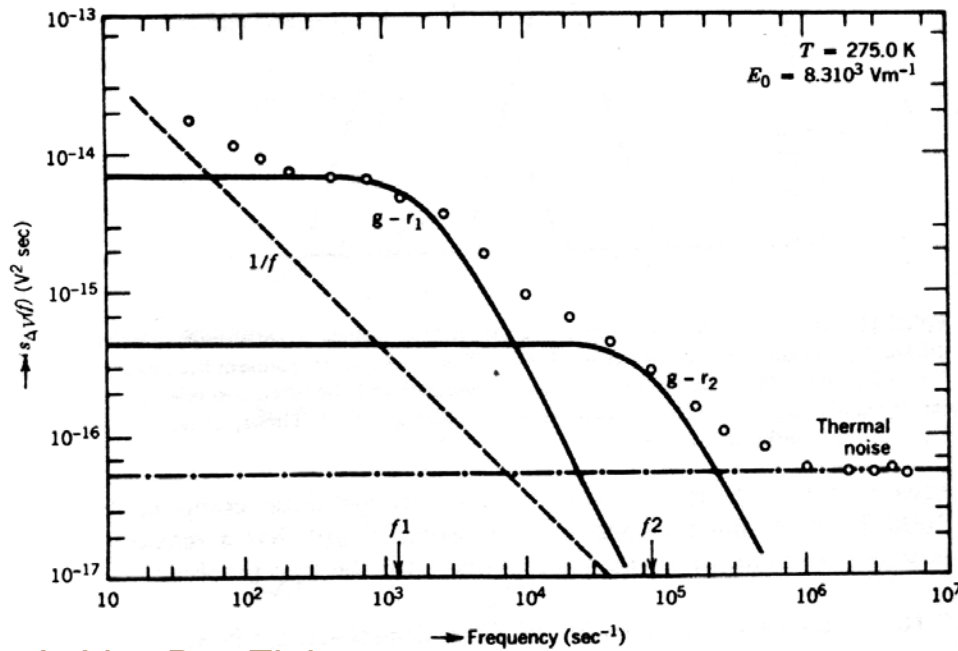
Technology 3

Current change: $\Delta I = \frac{I}{N_{TOT}} \times \text{Trap_Concentration}$

and time dependence: $\Delta T = \tau_0 e^{-t/\tau}$

Following the Generation Recombination, G-R, theory a noise is associated with this process. The noise being proportional to the square root of the Fourier transform the time dependence of the trapping process (Lorentzian function):

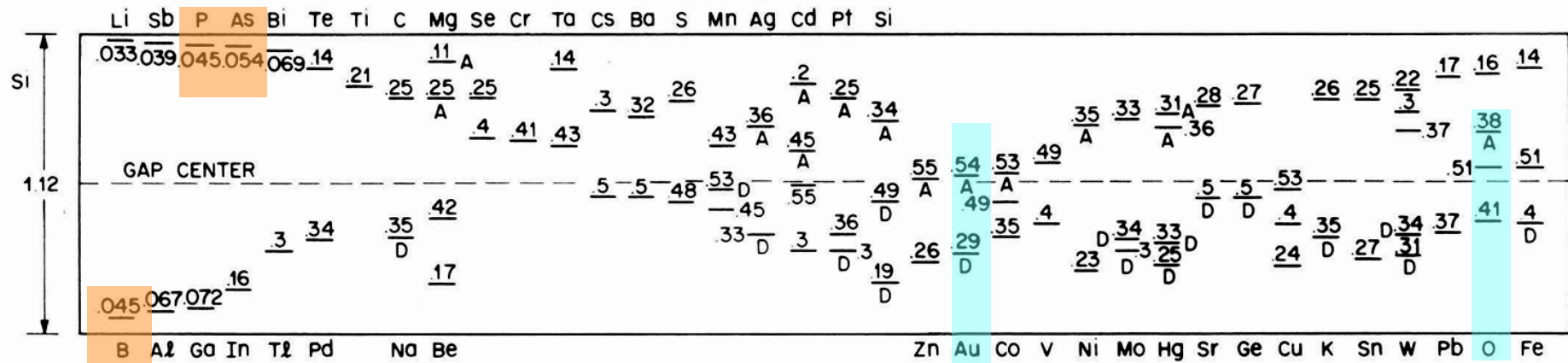
$$\overline{e_n^2} \div \frac{1}{1 + \omega^2 \tau^2}$$



A. Van Der Ziel

If several of such trapping centres are present with different concentration, characterized by different time constants, then the convolution of all the spectra leads to a 1/f behaviour.

Technology 4



= standard dopants, fast fast centers at room T

= trapping centers most efficient at room T

Now, let's come back a bit. A G-R centre close to the valence or conduction band, where close means having a distance in energy comparable to that of the phonon energy $k_B T$, will be empty most of the time (fast G-R), while a G-R centre close to the middle of the gap will be filled most of the time.

Both G-R centres do not have an effect on noise (one is always filled, the other always empty); the latter is useless, while the former is fundamental for the conduction mechanism.

Following this viewpoint, we can say that a good dopant must be chosen between those that are very very fast G-R centres at the operating temperature.

Technology 5

That is the reason why GaAs works well at deep cryogenic temperatures, while Si not:

Table 1 Energy gaps, masses and ionization energies for some semiconductors ^{18, 19}

	Si	Ge	GaP	GaAs	GaSb	InP	InAs	InSb
E_g at 4.2 K, eV	1.153	0.744	2.325	1.517	0.813	1.416	0.425	0.236
E_g at 300 K, eV	1.107	0.67	2.24	1.43	0.7	1.26	0.36	0.18
Donors	P, As, Sb		S, Se, Te					
m_n/m_0			0.34	0.04–0.07	0.047	0.077	0.025	0.012
E_d , eV	0.05	0.01	0.07	0.003		~0.003	0	0
Acceptors	B, Al, Ga		Zn, Cd					
m_p/m_0			~0.5	0.68	0.23	0.2	0.4	0.4–0.5
E_a , eV	0.05	0.01	0.04	0.02	0.037	0.05	0.007	0.008

Phonon energy:

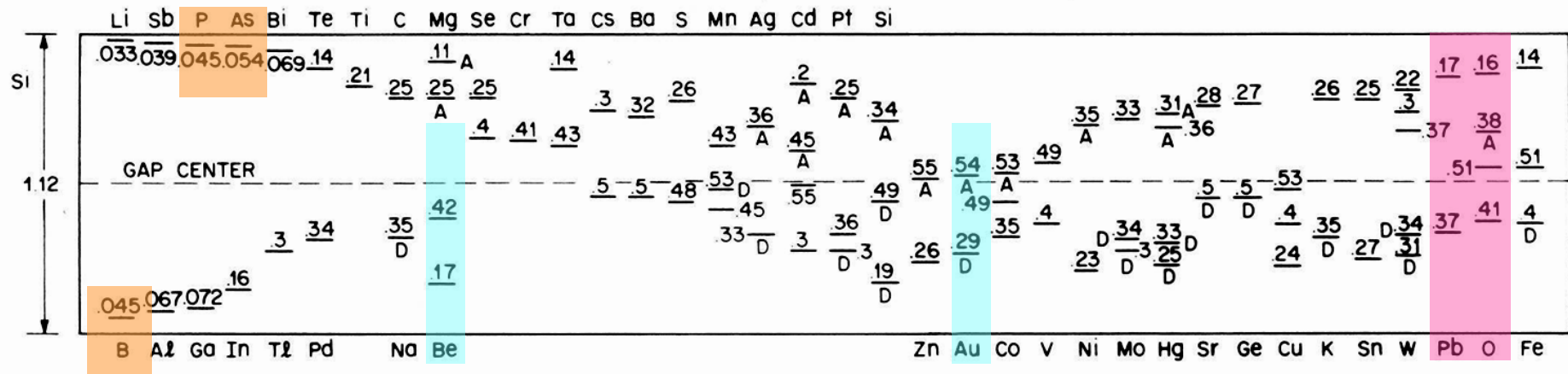
T[K]	$K_B T$ (meV)
300	26
77	6.7
4.2	0.4

Actually, best performances for Si – JFET are obtained in the range 100 – 150 K, where a compromise must be met between LF noise and maximum mobility, III – V compounds have no lower limit, practically.

B Lengeler Cryogenics V Agosto 1974 p 439

LTD-18, gpressina

Technology 6



= standard dopants, fast fast centers at room T

= trapping centers most efficient at room T

= trapping centers most efficient at LN

Starting from the middle of the gap, G-R always empty, going to the either of the 2 bands, G-R always filled, there will be some location in energy where the trapping/untrapping probability will equal: G-R centres with those energies will be more effective to contribute to LF noise.

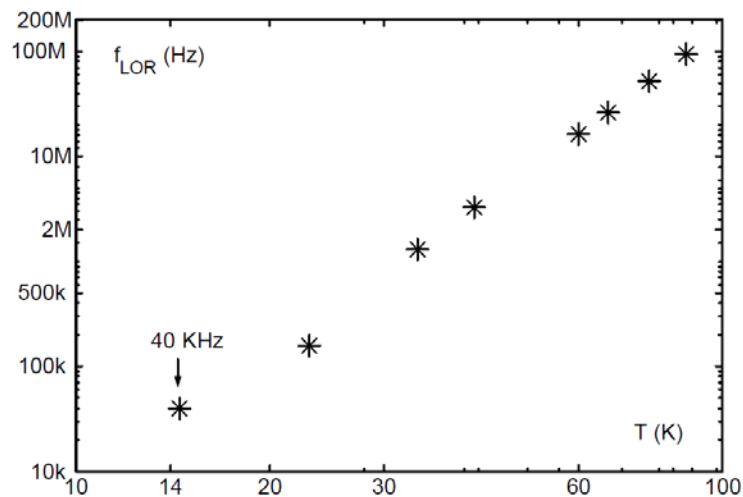
Increasing the temperature this energy, that with maximum noise effect, will move toward the middle of the gap, decreasing the temperature it will move close to the bands.

Technology 7

Indeed this is the case.

Lowering T below 80 K the noise increases apparently as if it were white in this plot since the upper bandwidth of the spectrum analyzer was 52 KHz.

(Thermal noise does not justify this behaviour unless it is considered hot electron effect at T much greater than room T)



Lorentzian frequencies versus temperature for the G-R noise from dopant atoms, after the parameters extracted from the data in **Figure 21**.

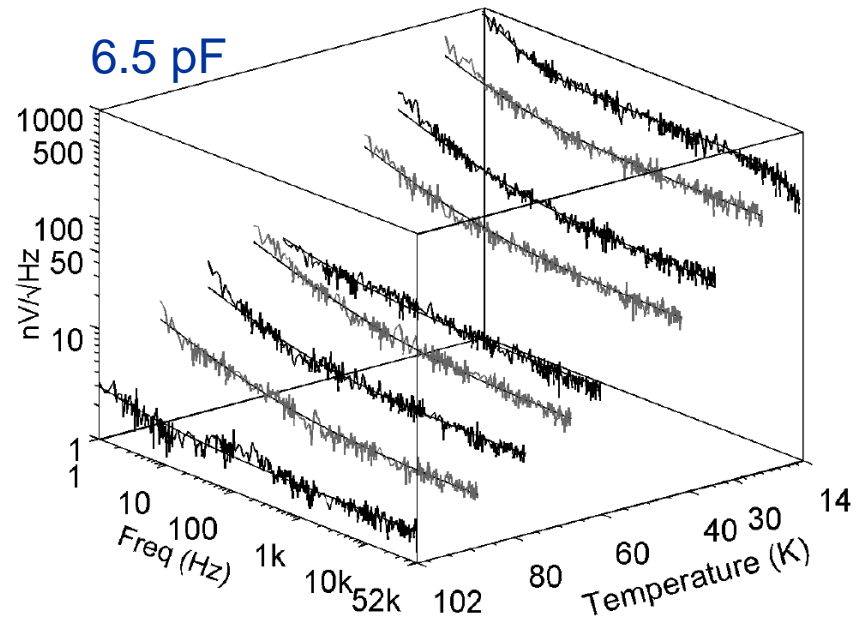


Figure 20: The 3D-plot of the noise spectra measured for the JFET MX11CD in the temperature range 15 K to 100 K. To each noise spectrum the fit is superimposed.

Only at about 14 K the corner frequency from G-R noise from donors is visible.

Here the corner frequency of G-R noise from donors is shown vs T . It enters the spectrum analyzer range only at 14 K.

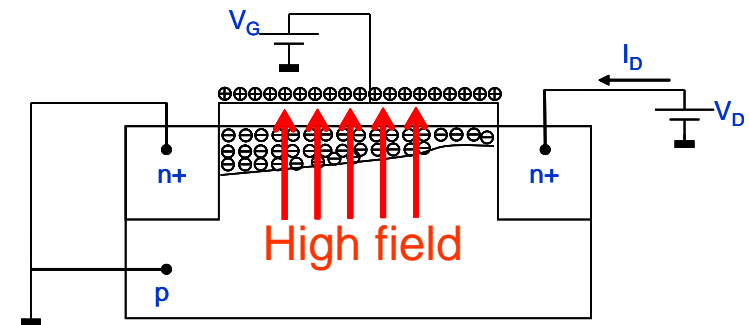
This rules out the use of JFET below 70 K unless a very special process is developed.

Technology 8

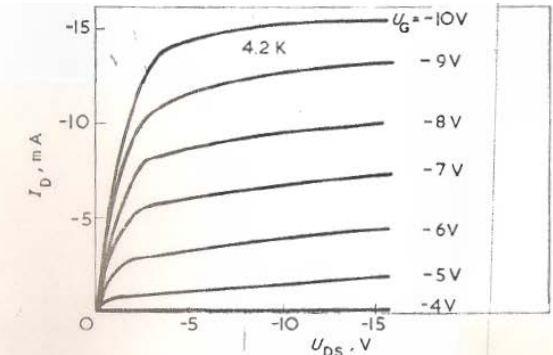
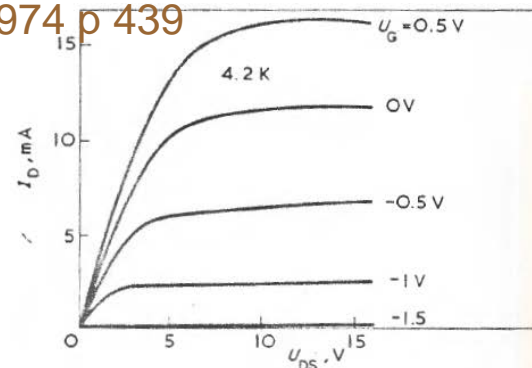
Working below 80 K is possible with III-V compounds such as GaAs, for their small donor ionization energy (3 meV), or Si-MOS, for the large transversal electric field that is able to free the carriers from dopants.

Although the carriers in the substrate are surely frozen out at 4.2 K, a conducting inversion layer may be built up between source and drain by field effect. In fact a small gate voltage can already produce very high electric fields, extracting charges from the source and the drain. In many *n*-channel depletion MOSFETs, the electric field produced

by the positive charges always present in the SiO_2 layer are numerous enough to generate a conducting channel by field effect. For MOSFETs to operate at 4.2 K it is essential that the source and the drain are heavily doped (10^{19} cm^{-3} — no carrier freeze-out), that the oxide layer is thin, and that the oxide layer overlaps with source and drain. Otherwise the electrical field is not strong enough to extract charges from the source and drain. We have investigated a great number



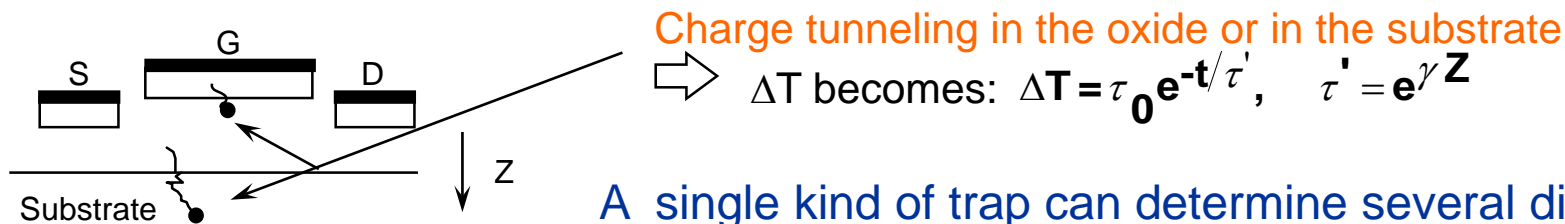
B Lengeler Cryogenics V Agosto 1974 p 439



Technology 9

Unfortunately, MOS and GaAs and, generally, III-V compounds work well at cryogenic temperatures, but their LF noise is not as small as that of Si JFET.

This is McWhorter model (1956) of LF: tunneling in the oxide



A single kind of trap can determine several different time constants depending on the distance of each trapping-atom of the species from the surface of separation between the oxide and the semiconductor.

This model seems to account well for the noise. A proof of this is the very different level of LF noise in PMOS and NMOS: the former shows a lower level that comes from the fact that holes can tunnel very little the oxide being slower and heavier of electrons.

Other models interpret the noise in term of mobility fluctuation or conductance fluctuation, see Hooge.

GaAs MESFET work well at deep cryogenic T. Unfortunately LF noise, that improves with T lowering, remains quite high and is a limit for several applications.

Low noise preamplifiers using GaAs MESFETs: D.V. Camin et al.

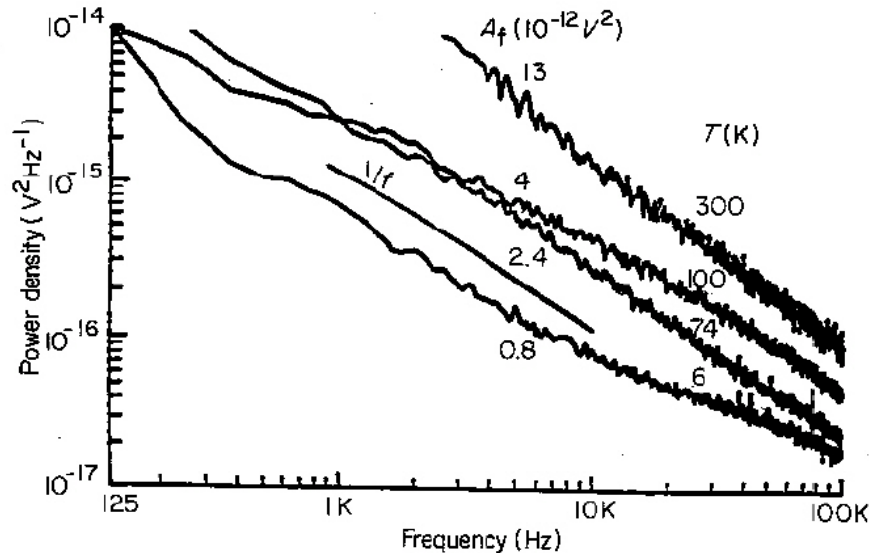


Figure 7 Noise power spectrum of the P35-1101-1 at different temperatures. Biasing current is 0.5 mA. There is a reduction of sixteen times when temperature decreases from 300 to 4 K

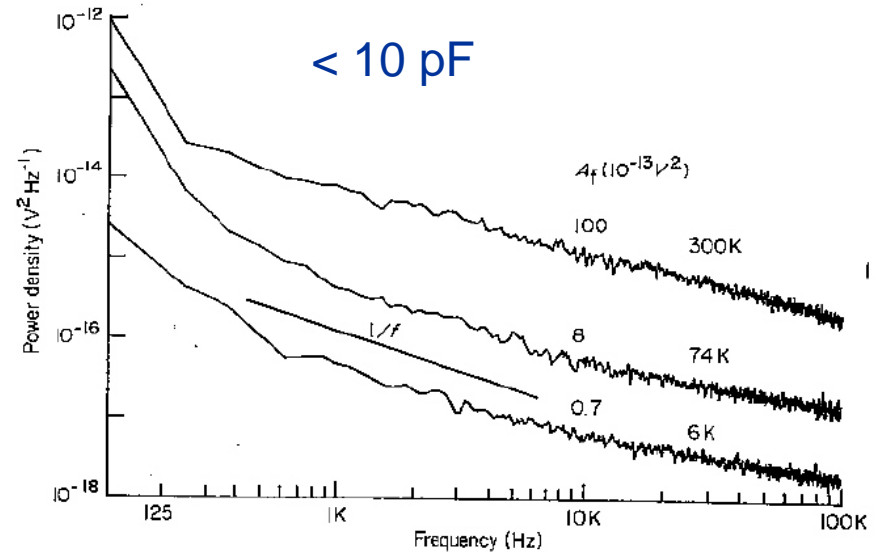


Figure 9 Noise power spectrum of the 3SK166 GaAs dual-gate MESFET at different temperatures. There is a reduction of more than two orders of magnitude when temperature decreases from 300 to 4 K

LF in GaAs comes from the crystal lattice imperfections (el-x traps), defects created between the semiconductor and metal surfaces, etc.

What about white noise with T ?

Thermal noise improves with lowering T , being proportional to T , but, generally, it improves less than expected.

That is due to the so-called hot-electron effect, namely, to the fact that the electron gas has a T larger than that of the lattice.

Here one example with a Si-JFET from room T down to 80 K.

Transconductance does not change so much and the input thermal noise has an improvement that is lower at large channel current, proving the hot-electron effect.

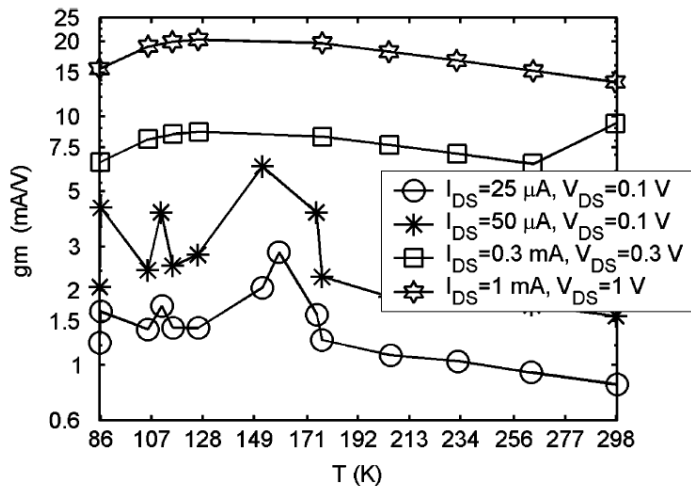


Fig. 10. Transconductance versus temperature for the SNJ450L109V_T0.6 at four different operating points.

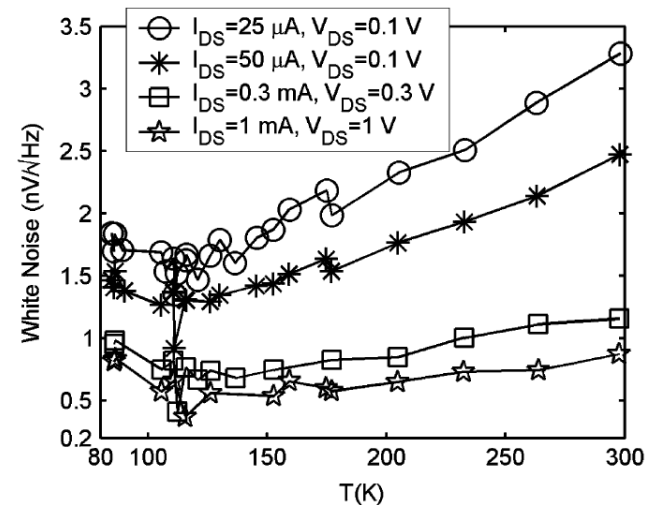


Fig. 13. Measured white noise for the SNJ450L109V_T0.6 for four different bias conditions.

Light sensitivity

Background reduction can be achieved also adding some signals which help in discriminating the events.

In this respect light produced in a crystal by an α particle (one of the main sources of background) is easily distinguished from γ , electrons and the like.

The crystal is coated with a reflecting foil which drives photons towards a thin sheet of Ge or Si which absorb them increasing its T. A thermistor or a whatever other sensor converts the increase of T in an electrical signal.

Depending on the properties of the crystal the light can be Cherenkov or scintillation.

